Carbon Capture Science & Technology 3 (2022) 100045

Contents lists available at ScienceDirect

Carbon Capture Science & Technology

journal homepage: www.elsevier.com/locate/ccst

Review

Impact of Surface Functional Groups and Their Introduction Methods on the Mechanisms of CO_2 Adsorption on Porous Carbonaceous Adsorbents

Ben Petrovic, Mikhail Gorbounov, Salman Masoudi Soltani*

Department of Chemical Engineering, Brunel University London, Uxbridge UB8 3PH, United Kingdom

ARTICLE INFO

Keywords:
CO_2
adsorbent
carbon
surface modification
functional groups

ABSTRACT

The utilisation of solid adsorbents for the selective removal of CO_2 from major emission points is an attractive method for post-combustion carbon capture due to the inherent potential for retrofit and cost-effectiveness. Although focus in the scientific community is often centred on extremely novel, high-performance and costly material development, the exploitation of carbonaceous adsorbents is another avenue of research proving to be extremely promising. This is even more pronounced when considering the abundance of carbon in various waste streams. The production of carbonaceous adsorbents, however, often requires significant post-treatments to enhance both the textural and physico-chemical properties of the adsorbent, as such, the incorporation of surface functionalities is unavoidable and can often lead to significant improvements to the associated CO_2 adsorption. This review aims to critically assess the various routes for surface modification of carbonaceous adsorbents and the implications these may have on the incorporation of surface functional groups. Subsequently, the adsorption mechanisms for CO_2 on surface-modified porous carbons are discussed in depth with consideration to the influence of the introduced functionalities. The review concludes with a detailed section on current modelling approaches such as the application of artificial intelligence, Monte Carlo, and Density Functional Theory simulations in this realm of research.

1. Introduction

Since the COP26 held in Glasgow at the end of 2021, over 90% of the worlds GDP and 90% of global emissions are now covered by a net-zero commitment, with most countries agreeing to strengthen their current targets to 2030. Alongside this, developed countries have progressed towards the delivery of the $100 billion climate finance goal by 2023. Additionally, 34 countries and five public finance institutions are to put an end to international support for the use of unabated fossil fuels in the energy sector which is currently valued at around $24 billion annually.

In 2019, the UK became the first major global economy to legislate for net-zero greenhouse gas (GHG) compared to 1990 levels by the year 2050 (Petrovic et al., 2021, Committe on Climate Change 2019). In November 2020 the UK government announced its 10-point plan which aims to "mobilise £12b of government investment and potentially three times as much from the private sector, to create and support up to 250,000 green jobs" (United Kingdom HM Government 2020). Annual anthropogenic CO_2 emissions primarily from the combustion of fossil fuels currently sit at over 40 billion tonnes, these emissions are instrumental in the global temperature rise observed today (Masoudi Soltani et al., 2021). The level of CO_2 in the atmosphere has increased from around 290 ppm during the preindustrial era to 409.8 ppm in 2019 (Lindsey, 2020). With around 85 % of global energy sourced from the combustion of fossil fuels (Younas et al., 2020), the implementation of carbon dioxide removal (CDR) technologies appears to be highly imperative. Carbon capture and storage (CCS) has been referred to as a "priority breakthrough technology" in their Green Deal, encouraging funding within the post Covid-19 recovery package (Masoudi Soltani et al., 2021, Renssen, 2022), and features as the 8th point of the UK's 10-point plan. Adsorption has seen increasing traction in the scientific community due to its high efficiency, more environmental-friendliness and low energy requirement relative to the more mature technologies such as solvent-based chemical absorption (Petrovic et al., 2020). Even with deployment of alternative energy sources that lack the associated CO_2 emissions, decarbonisation of the energy sector and industry is best described as a transitional period. CO_2 emissions will continue and without the use of CCS, the possibility of the commitments made during COP26 coming to fruition is questionable, especially within the given time constraints. Even after decarbonisation is achieved, the requirement for CO_2 removal from our atmosphere through processes such as direct air capture will not be removed. Processes such as adsorption alongside the materials currently being developed for such will continue to be essential in stabilising temperature increase to below 2°C.

* Corresponding author. Tel: +44(0) 1895 265884
E-mail address: Salman.MasoudiSoltani@brunel.ac.uk (S. Masoudi Soltani).

https://doi.org/10.1016/j.ccst.2022.100045
Received 19 February 2022; Received in revised form 24 March 2022; Accepted 24 March 2022

Nomenclature

Acronyms

GHG	Greenhouse Gas
CDR	Carbon Dioxide Removal
CCS	Carbon Capture and Storage
GCMC	Grand Canonical Monte Carlo
DFT	Density Functional Theory
AI	Artificial Intelligence
ML	Machine Learning
BET	Brunauer-Emmet-Teller
BG	Bagasse
SFG	Surface Functional Group
HW	Hickory Wood
FTIR	Fourier Transform Infrared Spectroscopy
XPS	X-ray Photoelectron Spectroscopy
AC	Activated Carbon
IAST	Ideal Adsorbed Solution Theory
TEPA	Tetraethylenepentamine
MEA	Monoethanolamine
DEA	Diethanolamine
PE	Polyethyleneimine
DETA	Diethylenetriamine
WA	Wood Ash
CEA	2-Chloroethylamine Hydrochloride
PDA	P-phenylenediamine
MWCNT	Multi-walled Carbon Nanotubes
DMF	Dimethyl Fumarate
HRTEM	High Resolution Transmission Electron Microscopy
HC	Hydrocahr
APTES	3-Aminopropyl(triethoxysilane)
MNP	Metal Nanoparticles
TOAB	Tetraoctylammonium Bromide
PET	Polyethylene Terephthalate
PAF	Porous Aromatic Framework
MPPA	Melamine-based Porous Polyamides
COF	Covalent Organic Framework
NPC	Nanoporous Carbon
MOF	Metal-organic Framework
LGB	Light Gradient Boosting
XGB	Extreme Gradient Boosting
GBDT	Gradient Boosting Decision Tree
DR	Dubinin-Radushkevich
DA	Dubinin-Astakhov

Symbols

Q_{st}	Isosteric Heat of Adsorption
T	Temperature
p	Pressure
R	Universal Gas Constant
1°, 2°, 3°	Primary, Secondary, Tertiary Amines
∀	Angstrom
E_b	Binding Energy
V	Adsorbed Amount
V_0	Micropore Volume
A	Adsorption Potential
E	Energy Constant
E_0	Characteristic Energy
β	Affinity Coefficient
q_t	Adsorbed Amount at time t
t	Time
k_{id}	Intra-particle (W&D) Diffusion Rate Constant

Solid porous carbons present good adsorption capacity for CO_2 gas at low concentrations and ambient temperature; however, their adsorption capacity decreases with increasing adsorption temperature. Therefore, surface modification is a critical method for increasing the CO_2 uptake capacity (Chiang and Juang, 2017) of solid porous carbons. Carbon-based porous adsorbents tend to be hydrophobic (Hao et al., 2013); therefore, heteroatom (O, N, and S) doping can be used to further enhance their hydrophobicity, improve their electron transfer rate, and modify the surface and pore structure (Ochedi et al., 2020, Singh et al., 2019). The presence of non-C elements and functional groups within carbonaceous frameworks and on the surface of carbons enhances their CO_2 capacity (Xia et al., 2011), and effectively improves their performance for CO_2 capture (Liu et al., 2012). These non-C elements and functional groups can be present depending on carbon precursor or any post-treatments (Gorbounov et al., 2021). Chingombe *et al.* (Chingombe et al., 2005) reported that functional groups in carbon structures can be manipulated using thermal or chemical treatments to produce sorbents for specific applications. Among different pyrolytic conditions, temperature is considered as the most important parameter since it controls both the final textural characteristics, and the surface functionalities of biochar alike (Singh et al., 2019). In addition, the heating rate and hold time markedly affect the physicochemical properties of porous carbons similar to the use of different chemical agents. When chemical agents are used, the final properties of the adsorbent depend on the type and amount of chemical agent. The final temperature of the chemical treatment is equally important in determining which functional groups form alongside effects to the adsorbent crystallinity and specific surface area.

Oxygen atoms typically combine with C atoms to form acidic or basic surface functional groups. The acidic character of porous carbons is typically attributed to groups such as carboxyl, lactone, phenol and lactol. Acidic functional groups can be removed using thermal treatments as most oxygen-containing groups decompose in the temperature range of 800–1000°C (Shafeeyan et al., 2010). On the other hand, two types of basic surface functional groups exist, *i.e.* groups with electron-donating properties and groups with π-electrons in their basal planes (Montes-Morán et al., 2004). Therefore, chromes, ketones, and pyrenes possess basic characteristics. Chemicals such as HNO_3, H_2SO_4, and H_2O_2 are often used to create O-rich functionalities on the surface of porous carbons (Singh et al., 2019). Carbon materials can be oxidized using gaseous or aqueous solutions; in addition, high and low temperatures lead to the incorporation of weak and strong acidic groups, respectively (Creamer and Gao, 2016), alongside the removal of hydrophilic groups (Plaza et al., 2009). Nitrogen-enriched porous carbons can be produced by introducing N in the carbon precursors, using different N-containing activating agents or by exposing carbons to N compounds at elevated temperatures (Pietrzak, 2009). Sulphur-doped carbons can be as effective as N-doped carbons. Sulphur incorporated into aromatic carbon rings has been demonstrated to enhance CO_2 adsorption *via* acid–base interactions within the micropores (Chiang and Juang, 2017). Additionally, sulfo-groups, sulfoxides and sulfones can attract CO_2 *via* polar interactions (Seredych et al., 2014). Based on the outlook set out in the preceding paragraphs, it is evident that an in-depth understanding of the impact of such functionalities on the performance of carbonaceous adsorbents is of major significance.

1.1. Motivation and Paper's Roadmap

The effects of climate change and the global mobilisation of the scientific community to tackle both the causes and symptoms can be seen in the increasing attention; in the context of this paper it can be seen in the number of publications and citations within the field. In the last 40 years, publications featuring 'CO_2' and 'adsorption' have increased from 54 in 1981 to over 3500 in 2021 as can be seen in Figure 1. Similarly, publications featuring "Surface Modification" and "Carbon" has increased from 5 to over 700 in the same period (Figure 1).

With a view to buttress our recent publication (Petrovic et al., 2020), this work seeks to scrutinise the literature published in the context of

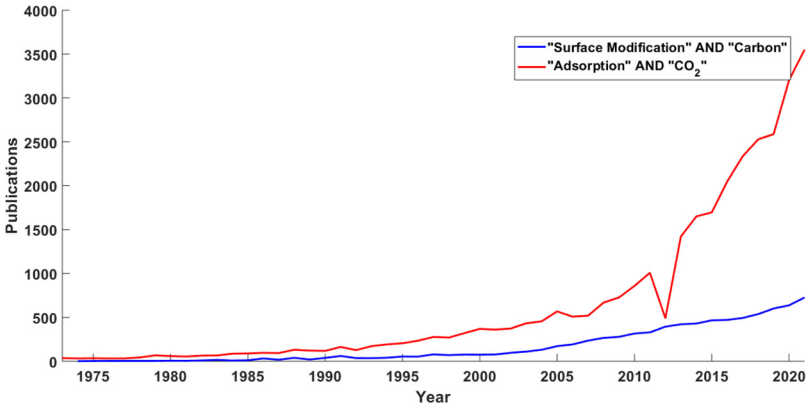

Figure 1. Publications indexed on SCOPUS by publication year.

surface modification of carbonaceous adsorbents and their applicability for the selective removal of CO_2 from gaseous streams. As such, this review first discusses the diffusional mechanisms that carbonaceous materials present. Thereafter a description of the mechanisms presented by various surface heterogeneities and their observed interactions in the presence of moisture is given followed by an assessment of the various processes available for introduction of such surface moieties. Finally, focus is shifted to the implementation of novel methods such as Grand Canonical Monte Carlo (GCMC) simulations, Density Functional Theory (DFT), Artificial Intelligence (AI) and Machine Learning (ML) for assessing the influence of specific surface functional group on CO_2 adsorption.

2. Diffusion Mechanisms

Four mechanisms exist for the transport of mass through porous materials, *i.e.* molecular or bulk diffusion, Knudsen diffusion, surface diffusion, and Poiseuille flow (Do, 1998, Kast, 1985, Lightfoo et al., 1960). These mechanisms do not occur independently and the structure of the adsorbent can cause synergistic or competitive relationships between these mechanisms (Suzuki, 1991). The classification of micro-, meso- and macropores is primarily based upon the forces that control the adsorption mechanism. Surface forces are dominant in micropores, wherein fluid particles never escape the surface force field even in the pore centre (Wilcox, 2012). For mesopores, the dominant force is the capillary force, whereas macropores are critical for bulk fluid transport. When the size of the adsorbate molecule is similar to that of the pores (steric hinderance), the diffusion rate is limited. Consequently, diffusion becomes an activated process, wherein the fluid diffuses across the surface by hopping between adjacent "potential-well" sites on the surface; an activation barrier is associated with each hop (Wilcox, 2012). When a degree of adsorbate mobility exists on the adsorbent surface, typical when multiple layers of adsorbate exist, they can migrate (Knaebel, 2008). This surface diffusion process has been reported to contribute more to intraparticle diffusion than pore diffusion (Suzuki, 1991). Knudsen diffusion occurs when the mean free path of the molecules is greater than the pore diameter and is typical within mesopores, where interactions between the fluid and surface often more frequent. Surface diffusion and capillary effects can also affect the transport behaviour in mesopores. For macropores, mass transport typically occurs *via* bulk or molecular diffusion, which is synonymous with pore diffusion.

Different carbonaceous sorbent precursors and their respective activation methods impart different properties to pyrogenic carbons. Therefore, the primary aim in development of the adsorbent material is to achieve minimal diffusional resistance for the adsorbate until adsorption can occur in the meso- or micropores (Creamer and Gao, 2016) hence, accelerating the CO_2 adsorption kinetics (Hao et al., 2013). CO_2 is typically adsorbed *via* i) bulk diffusion: CO_2 molecules diffuse from the bulk gas phase to the external surface of the sorbent; ii) film/boundary layer diffusion: CO_2 molecules diffuse through the gas film around the sorbent; iii) intraparticle diffusion: CO_2 molecules diffuse in the pores in the bulk of the sorbent; and iv) surface adsorption: CO_2 molecules interact with the active sites on the internal surface of the sorbent (Raganati et al., 2019, Raganati et al., 2020). Before carbonaceous precursors undergo gasification or pyrolysis, they present narrow and typically slit-like pores; hence, gases are strongly adsorbed at low pressures due to an enhancement of adsorption potential due to overlap of the force fields of opposite pore walls (McEnaney, 1988), any constrictions in the microporous network result in activated diffusion effects at low temperatures when the adsorbate has insufficient kinetic energy to penetrate the micropore space (McEnaney, 1988) as such, an activation energy is required for the diffusion of gases (Creamer and Gao, 2016). In the case of microporous carbons, adsorption occurs by primary or micropore filling, Dubinin and his group modelled the process using Polanyi potential theory; however, they identified that empirically the characteristic adsorption curves could be linearized using the Dubinin-Radushkevich (DR) equation (McEnaney, 1988, Dubinin, 1975, Dubinin, 1989):

$$V = V_0 e^{-\left(A/E\right)^2}$$

Where V is the amount adsorbed at relative pressure P/P_0, V_0 is the micropore volume, $A = RT \ln P/P_0$ is the adsorption potential where R is the gas constant and T the absolute temperature, and E is the energy constant. Dubinin also showed that E could be factorised into a characteristic energy (E_0) relating to the adsorbent and an affinity coefficient (β) which is a constant for a given adsorptive (McEnaney, 1988). The DR equation although linear for some carbons over a wide range of pressures, some deviations can be found for other carbons and in these cases the Dubinin-Astakhov (DA) equation was proposed which simply replaces the exponent, 2, in the DR equation with an adjustable constant, n (McEnaney, 1988, Dubinin, 1975). The value for n can give indication to the distribution of micropore size with $n < 2$ observed in carbons with a wide range of micropores or nonhomogeneous structure (Dubinin, 1989), above 2, this is often indicative of inactivated or slightly activated carbons with a narrow micropore range; further deviations from the DR equation can be a result of activated diffusion and this is usually exhibited by downward deflections in the DR plot at low relative pressures (McEnaney, 1988). When the pores are widened during subsequent treatments, sorption follows bulk or Knudsen diffusion principles, for which the gas transport rate is limited by the diffusion into and out of a feeder pore system of larger pores, such as mesopores (Ravikovitch et al., 2000) and macropores.

For porous carbons, diffusion effects can be extremely important and to give insight into the mass transfer mechanisms a specific adsorbent may present. The intra-particle diffusion model postulated by Weber and Morris can be used to identify consecutive stages of mass transfer during the adsorption process (Álvarez-Gutiérrez et al., 2017, MORRIS and

WEBER, 1964):

$$q_t = k_{id} t^{1/2} + C$$

Where q_t is the amount adsorbed at a time t, k_{id} is the intra-particle diffusion rate constant and C refers to the thickness of the boundary layer. According to this model, when plotting q_t vs $t^{1/2}$, a straight line passing through the origin indicates that the rate-controlling mechanism is the intraparticle diffusion. However, in the case that the plot present multi-linearity, the adsorption mechanism consists of a number of stages. Typically this follows three steps, the first corresponding to the external or bulk diffusion, the second being the intra-particle diffusion and the third is generally accepted as the equilibrium stage (Álvarez-Gutiérrez et al., 2017, Loganathan et al., 2014). The slope of the line is defined as the rate parameter, $k_{id,i}$, with the lowest slope representing the rate-determining step.

Montagnaro et al. (2015) reported that ACs featuring mesopores presented lower intraparticle diffusion resistance than those featuring only micropores, although macropores have also been demonstrated to be beneficial for CO_2 diffusion (Wang et al., 2017). The presence of meso- and macropores can enhance diffusion into micro- and ultra-micropores by shortening diffusion paths (Manyà et al., 2018). The CO_2 adsorption capacity of carbonaceous materials decreases with increasing adsorption temperature and a decreasing CO_2 volumetric fraction owing to the exothermic nature of the CO_2 adsorption process (García et al., 2011). The dynamic diameters of CO_2 and N_2 are 0.33 and 0.364 nm, respectively (Wang et al., 2011), which suggests that pores of 0.5-0.6 nm should be ideal for the selective capture of CO_2 (Chiang and Juang, 2017). The increase in narrow microporosity of C-based adsorbents can increase their CO_2 uptake capacity under ambient conditions (Sevilla and Fuertes, 2011, Wickramaratne and Jaroniec, 2013). At 1 and 0.1 bar (100 and 10 kPa), pores smaller than 0.8 and 0.5 nm, respectively, contributed to CO_2 adsorption the most (Presser et al., 2011). Having said this, a pore size range of approximately 0.5 – 0.8 nm is often identified experimentally as the ideal for CO_2 separation. Martinez *et al.* (Martín-Martínez et al., 1995) prepared a series of porous carbons from anthracite and evaluated their CO_2 adsorption mechanism based on the size and shape of the pores. They reported that narrow micropores were filled *via* physical adsorption; however, wider micropores facilitated surface adsorption and presented rectilinear adsorption isotherms. Ello et al. (2013) and Zhu et al. (2014) suggested that the micropore volume plays a crucial role in facilitating high CO_2 adsorption capacities. High-surface area carbons were produced in both studies; however, the adsorption capacities of the carbons with the largest specific surface areas were lower than those of the carbons with higher micropore volumes.

3. Molecular Interaction Mechanisms for CO_2 Adsorption

Carbon capture by solid adsorbents primarily requires the selective separation of CO_2 from N_2. The adsorbate, CO_2, is often preferentially adsorbed on the carbonaceous surface due to its greater polarizability and quadrupole moment (McDonald et al., 2011); the quadrupole moment is of the utmost importance when evaluating SFGs and the mechanism of attractions between the CO_2 molecule and the adsorbent surface. Generally speaking, CO_2 adsorption by carbons is governed by the London dispersion forces (Petrushenko et al., 2021), a subdivision of van der Waals intermolecular forces predominant in non-polar media. The high atomic density of a carbonaceous sorbent (which yields strong dispersion force attractions between the surface carbon atoms and the highly polarisable oxygen in CO_2) is the primary reason for such interaction. Aside from the dispersion and induction of CO_2 to the surface of carbons, surface properties also play an important role (Adsorbents, 2003) (e.g. specific surface area, pore size distribution and porosity) as well as process conditions such as temperature and pressure (Adelodun et al., 2015) which are major contributing factors. On an operational level, the route in which the gas contacts the adsorbent particles is instrumental in the kinetics of the adsorption process. The addition of heteroatoms in the form of SFGs to the carbonaceous material along with the associated secondary effects leads to a significant manipulation of the adsorbent properties. The implications these modifications may have on the adsorption mechanism and the derived process must be well understood for the successful deployment of adsorption-based CCS. the properties of the adsorbent.

3.1. Physical Adsorption

As mentioned previously, physisorption is governed by van der Waals interactions and electrostatic forces. Van der Waals forces are present in all systems but electrostatic interactions only occur in systems that contain permanent charges (*i.e.* sorbents with ionised-SFGs) (Wilcox, 2012). Van der Waals forces can be subdivided into Keeson interactions, Debye forces, and London dispersion forces; the sum of the van der Waals and electrostatic forces is the overall intermolecular force between the adsorbent and the CO_2 molecule.

In highly porous carbons, adsorption occurs primarily on the pore walls, or at specific sites inside particles (McCabe et al., 1993). Separation occurs because of variations in the weight, shape or polarity of molecules, which can result in stronger interactions between the molecule and the adsorbent surface and lead to a greater affinity towards the specific molecule. This exploitation of the differences between interaction strengths is the basic principle of adsorption (Sinnott and Towler, 2009). The distinction between physisorption and chemisorption can be observed experimentally using magnitudes of the isosteric heat of adsorption, Q_{st}. The heat of adsorption is typically low for physisorption (8 – 40 kJ mol^{-1}), which is equivalent to the condensation heat of the adsorbent, and high for chemisorption (40 – 800 kJ mol^{-1}), which is equivalent to the enthalpy of reaction (Nakao et al., 2019, Chang and Chen, 2006). The addition of heteroatoms in the form of SFGs significantly impacts the polarizability of the sorbent, which has the potential to increase the observed isosteric heat of adsorption to above values typical for physisorption of carbon dioxide (Youk et al., 2020) The isosteric heat of adsorption is the ratio of the infinitesimal change in adsorbate enthalpy to the infinitesimal change in the amount adsorbed and gives a direct measurement of the strength of the interaction between the molecules of the adsorbate and adsorbent surface (Serafin et al., 2017). The Clausius-Clayperon equation is used to calculate Q_{st}:

$$Q_{st} = -R\left[\frac{\partial \ln p}{\partial\left(\frac{1}{T}\right)}\right]_{q_e}$$

Where Q_{st} (kJ mol^{-1}) is the isosteric heat of adsorption, q_e is the adsorption capacity (mmol g^{-1}) at temperature T (K) and R (8.314 J mol^{-1}•K^{-1}) is the universal gas constant. In order to calculate Q_{st}, isotherms generated at two temperatures are required and are often evaluated at 0°C and 25°C. the value of Q_{st} gives the average binding energy between the adsorbate and functional groups present on a specific surface, but also facilitates further verification of the adsorption mechanism (Alabadi et al., 2015). Physisorption by carbons is typically driven by intraparticle diffusion into the pores; therefore, pore size and distribution are key factors (Adelodun et al., 2015). Sevilla et al. (2012) and Yuan et al. (2020) reported that the capacities of the porous carbons they prepared were exclusively the results of high volumes of narrow micropores and were not related to the surface areas, pore volumes, or presence of heteroatoms. The significance of the heteroatoms was more pronounced when the selective adsorption of CO_2 from various mixtures was considered.

Given the negligible variations in the dynamic diameters of CO_2, O_2 and N_2 (0.33, 0.346 and 0.364 nm, respectively), Wang et al., 2011) identified the selective adsorption mechanism of CO_2 using several sim-

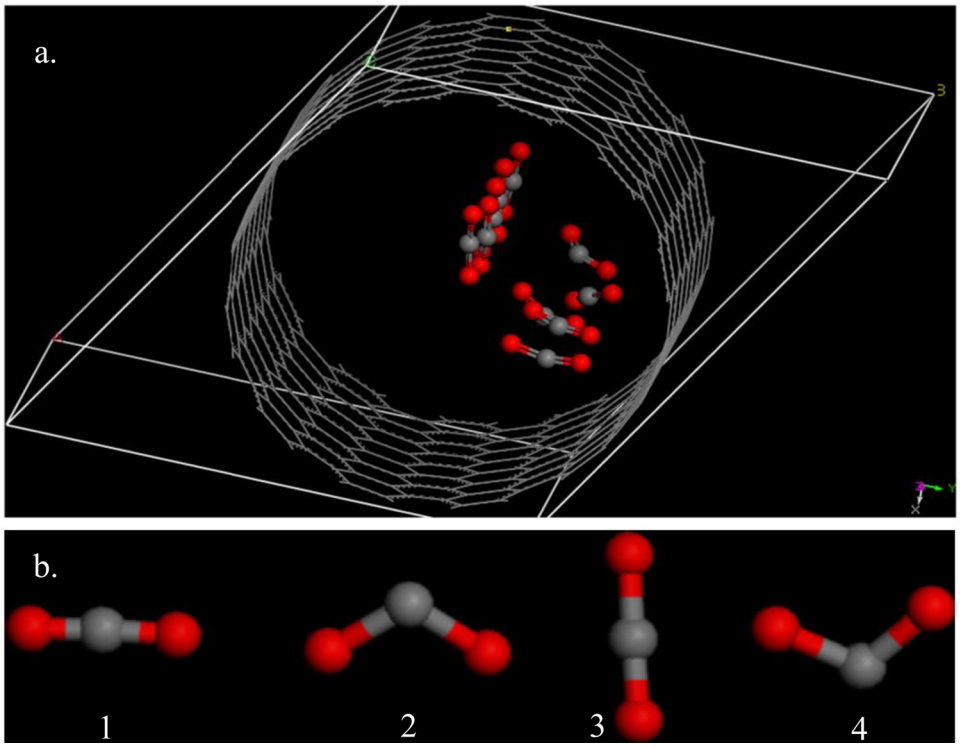

Figure 2. a. State of molecular CO_2 adsorbed in the nanopore (diameter = 0.8 nm); b. Possible adsorption configurations of molecular CO_2. Reproduced from Ref. (Martín-Martínez et al., 1995)

ulations. CO_2 is a linear (O=C=O) nonpolar molecule and has no molecular polarity (Chiang and Juang, 2017). The simulation results indicated that if a CO_2 molecule was located in the centre of a 0.8 nm nanopore, symmetrical forces acted on its C=O bonds and the CO_2 molecule maintained its linear shape (Yuan et al., 2020). If the CO_2 molecule was located near a nanopore wall, the O=C bonds were polarized instantaneously owing to the high London dispersion force between the O atom of the bond and the C atom of the active sites. This resulted in asymmetrical forces acting on the C=O bonds and caused the bending of the CO_2 molecule. Two additional orientations were identified and all four configurations are illustrated in Figure 2. The second and fourth configuration presented certain polar and dipole moments, and these polarized molecules would be chemisorbed on active carbon sites to produce surface C-O complexes, such as lactone, carbonyl-type, furan and heterocyclic O-containing groups. With respect to physical adsorption, polarized CO_2 molecules strengthened the London dispersion and overall van der Waals forces, which led to stronger adsorption forces and higher selectivities (Zhao et al., 2012, Wang and Yang, 2012). Another often observed phenomenon for carbon capture by solid sorbents is the prevalence of ultramicroporous structures. Porosity of this order is preferred as it allows for the simultaneous interaction between the CO_2 molecule and each side of the pore wall (Patel et al., 2017). This phenomenon occurs due to an overlap in the potential energy surfaces leading to an increase in the binding energy reaching a maxima in the region of 0.7 – 0.8 nm (Wang et al., 2017).

3.2. Chemical Adsorption

Chemisorption is typically characterized by the formation of new bonds with a binding energy greater than approximately 0.5 eV (8.01×10^{-20} J) per molecule (Spanjaard and Desjonqueres, 1990). Chemisorption is described in some cases as “specific” adsorption, in which the adsorbate (CO_2) reacts with a specific site (Rouquerol et al., 2013) (*e.g.,* CO_2 forms bonds with different N-containing groups, whereas N_2 does not (Webley and Danaci, 2019)). The chemical properties of carbons that affect the feasibility and extent of chemisorption are determined by the chemical heterogeneity of their surface. The surface chemical heterogeneity depends on the presence of heteroatoms, such as O, N, and S. The specific form and respective quantity of heteroatoms, depends on the modification method and/or material the carbon is derived from. Basic groups with an immediate affinity for CO_2 improve the interactions with CO_2 but not to the point where adsorption becomes entirely chemisorption (Chiang and Juang, 2017). However, this interaction becomes more noticeable at high temperatures, which indicates that the adsorption mechanism is not entirely physical (Yong et al., 2002).

For instance, increasing the (Lewis) basicity of the sorbent surface increases the affinity of the (Lewis) acidic CO_2 molecule for the sorbent surface (Chiang and Juang, 2017). Oxygen-containing functionalities that form during oxidative treatments induce an acidic character, and therefore, impart electron-acceptor properties to the adsorbents. Conversely, N-containing functionalities typically possess an inherently basic character. This confers electron-donor properties to these functionalities, which serve as attractive adsorption sites for the electron-deficient C-atom in the CO_2 molecule (Adelodun et al., 2015). With respect to the specific N-functionalities produced during treatments, amines, imines, imides, amides and nitriles will be the predominate species produced at low temperatures. When increasing temperature to above 450°C, the aromatic species such as pyrrolic and pyridinic-N would take prevalence although there will be a gradual conversion of pyrrolic-N to pyridinic-N above 600°C (Pels et al., 1995). Both O- and N-SFGs can beneficially influence the adsorption of CO_2, but the presence of O prior to N-doping can significantly improve the effectiveness of N-functionalization (Figure 3).

At an adsorption temperature of 20°C and often at low pressures (1 bar), physisorption in micropores is the dominant mechanism that controls the adsorption of CO_2. Low pressure (1 bar) CO_2 adsorption behaviour has been shown to be almost independent of BET surface area (Srinivas et al., 2012, Hu et al., 2011). However, at temperatures around 120°C, the N-content of carbons plays a signification role in the chemical adsorption of CO_2 *via* simple acid–base interactions (Zhang et al., 2014). This was attributed to higher adsorption temperatures resulting in higher CO_2 transport rates through the pore

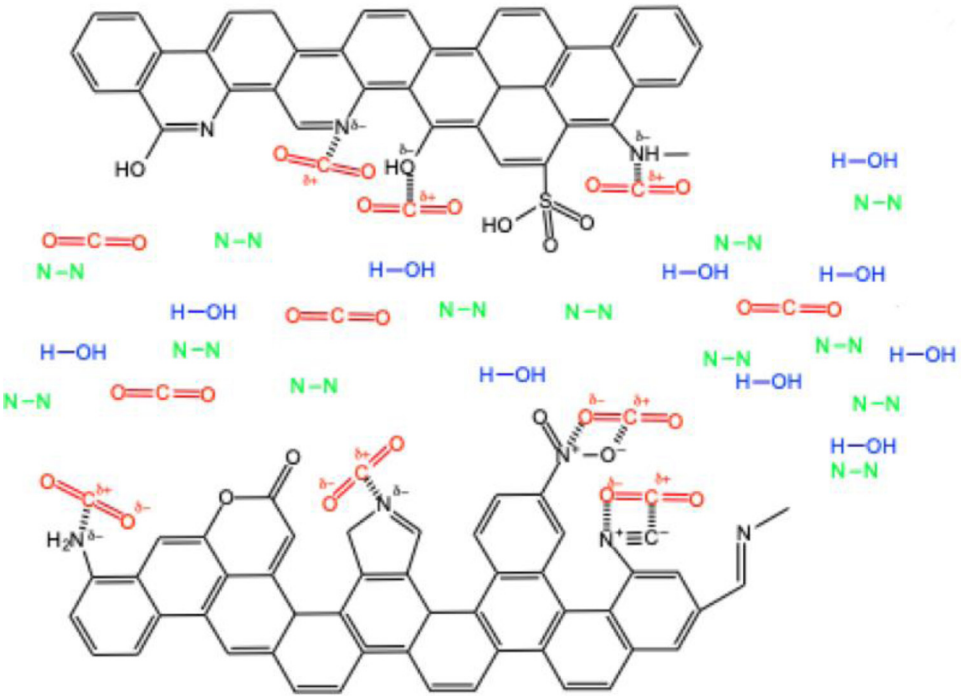

Figure 3. Example of chemisorption mechanisms of CO_2 by some carbon SFGs from flue gas reproduced from (Petrovic et al., 2020).

structure and enhancing the accessibility of the active sites, which led to an increase in deactivation rate (Zhang et al., 2014). Consequently, the initial adsorption rate decreases as the major adsorption driving force shifts from physical to chemical adsorption with increasing adsorption temperature (Zhang et al., 2016, Hosseini et al., 2015, Mulgundmath et al., 2012). At 120°C, the dominant driving force is chemical adsorption, which is promoted by the presence of N-functional groups (Yang et al., 2012, Plaza et al., 2007).

The Q_{st} values determined by Alabadi et al. (2015) using CO_2 adsorption isotherms based on the Clausius-Clapeyron equation confirmed the interaction strength between CO_2 molecules and the surface of nitrogen-doped carbons. In the range of 21.7 – 62.9 kJ mol^{-1}, Q_{st} demonstrated that the N- and O-functionalities of porous carbons can interact significantly with CO_2 (Rabbani and El-Kaderi, 2011). Furthermore, Q_{st} can be regulated by manipulating the contents of both N- and O-SFGs, which suggested that both physisorption and chemisorption occurred concurrently. The exceptional performance of one of the sorbents prepared by Alabadi et al. (2015) was attributed to its relatively small pore volume Luo et al. (2013) and large number of non-C elements such as electron-rich N- and O-atoms with strong dipole-quadrupole interactions with CO_2, significantly increasing the enthalpy of CO_2 adsorption (Lu et al., 2012). Increases in Q_{st} with adsorbate loading can also elucidate to the adsorption mechanism. Hu et al. (2017) tracked Q_{st} as CO_2 loading increased, they observed a decrease from 15 to 14.5 kJ mol^{-1} on MWCNTs as the adsorbed amount increased from 0.07 to 0.15 mmol g^{-1} as the interactions became weaker as the strong adsorption sites are occupied. On the amine-grafted derivative, Q_{st} was shown to increase with CO_2 loading, suggesting the dominant mechanism is indeed chemisorption in agreement with Hu et al. (2017), Alhwaige et al. (2013).

The mechanisms by which CO_2 is adsorbed because of these functional groups is as complex as the methods used to introduce them and can be assessed by classifying them based on their innate heteroatoms. However, these groups cannot be assumed to be entirely independent of one another. Delineation of such synergistic or potentially inimical relations in the context of CO_2 adsorption is difficult to achieve and still requires significant scrutiny.

3.3. Oxygen Containing Functional Groups

Oxygen-containing groups control two properties of C-adsorbents: hydrophobicity/hydrophilicity and acidity/basicity; the degree of hydrophilicity is influenced by the amount of polar O-groups present (Saha and Kienbaum, 2019) since pristine carbon is hydrophobic (Menéndez-Díaz and Martín-Gullón, 2006). Hydrophilicity however, is detrimental for CO_2 adsorption as it increases the competition for active adsorption sites between CO_2 and moisture in the flue gas (Saha and Kienbaum, 2019). Groups are classified as acidic, basic or neutral based on their available free π-electrons and thermal refractivity attributed to their inherent bond energies as opposed to conventional pH levels (Shafeeyan et al., 2010, Lahaye, 1998). The oxidation of carbons introduces different O-functionalities, and imparts electron-acceptor properties to the surface (Vagner et al., 2003). The -COOH, lactone, lactol and phenol groups contribute to surface acidity, whereas pyrone, carbonyl, benzopyran, diketone/quinone, ether, ketone and alcohol groups are responsible for surface basicity (Montes-Morán et al., 2004, Saha and Kienbaum, 2019, Goel et al., 2015, Lopez-Ramon et al., 1999).

Tiwari et al. (2016) postulated that the highest CO_2 adsorption capacity achieved in their epoxy resin-derived carbons was due to the greater content of O-containing basic groups. Babu et al. (2017) reported that both -COOH and -OH groups led to considerable improvements in adsorption capacity at ambient pressures whilst not realizing any further improvements after subsequent N-doping. Nitrogen-SFGs are not the only species that present Lewis basic character; O-containing groups such as carbonyls, alcohols and ethers contain an electron-donating O-atom that can participate in electrostatic interactions with CO_2 (Liu and Wilcox, 2013, Plaza et al., 2013), thereby enhancing the adsorption of polarisable species such as CO_2 *via* Lewis acid-base interactions (Kazarian et al., 1996). The electron transfer between carbonyl and CO_2 is reported to present a greater electron transfer than between benzene and CO_2 (Nelson and Borkman, 1998). Plaza et al. (2013) reported strong Lewis acid-base interactions between CO_2 and -COOH groups. Of the basic O-containing groups, pyrone is often studied; pyrone-like structures are combinations of non-neighbouring carbonyl and ether-O atoms at the edges of a graphene layer (Montes-Morán et al.,

2004). The basicity of pyrone can be explained by the stabilisation of its protonated form *via* electronic π-conjugation throughout the sp^2 skeleton of the carbon basal plane (Montes-Morán et al., 2004, Saha and Kienbaum, 2019, Fuente et al., 2003). The basicity of the -OH group is often reported and is frequently shown to positively impact the adsorption of CO_2 (Singh et al., 2018, Tiwari et al., 2017). Liu *et al.* have reported that -OH and carbonyl groups affect the CO_2 adsorption due to their high electron densities (Liu and Wilcox, 2012). The interactions between -OH groups and CO_2 can also be described by the potential of electron donation to CO_2 as a result of the high electrostatic potential (Ma et al., 2018). Moreover, -OH groups have been shown to affect CO_2 adsorption through H-bond interactions (Ma et al., 2018, Ren et al., 2010); a linear relationship between the contents of the group and CO_2 adsorption was reported by Ma *et al.* (Ma et al., 2018) at adsorption conditions of up to 0.5 bar at 25˚C. Such linearity was lost when increasing adsorption pressure from 0.5 to 1 bar. Yuan *et al.* (Yuan et al., 2020) were able to successfully identify that the -OH functional group significantly enhances the interactions between polyethyelene terephthalate (PET) derived microporous carbon and CO_2. Moreover, they discovered that ether groups played no role in CO_2 adsorption, while ester groups were shown to reduce the CO_2 capacity as a result of pore blocking. Q_{st} for the -OH functionalized system increased from 31.13 (0.323 eV) for the pristine system to 42.13 kJ mol^{-1} (0.437 eV). Adsorption energies for -OH groups and CO_2 have been reported by Ma et al. (2018) as 14.88 (0.154 eV) and 12.11 kJ mol^{-1} (0.126 eV), depending on the orientation of the CO_2 molecule.

As a general guideline, O-containing functional groups are produced during the oxidation of organic structures (Guo et al., 2020) during the various chemical or physical activation procedures. Acidic groups such as carboxylic, carbonyl, lactonic and phenolic groups will form at relatively low temperatures when oxidizing with HNO_3, H_2O_2, H_3PO_4 or H_2SO_4 (Rajapaksha et al., 2016). Plaza *et al.* reported that liquid phase oxidation introduces a greater amount of O, mostly as carboxylic groups that are absent in gas phase oxidised samples that contain mostly ether and carbonyl functionalities (Plaza et al., 2013). For gas phase oxidations below 673 K the formation of C-O complexes is favoured however above this temperature, the decomposition of these surface complexes and gasification of the C become the predominant reactions (Plaza et al., 2013, Bansal and Goyal, 2005). NaOH activation has been shown to introduce extraordinary strong surface basicity compared to H_3PO_4 (Guo et al., 2020) using the same activation temperature of 850˚C. Increases in O-concentrations can also be achieved with HNO_3 activation in the form of predominantly -OH and carbonyl groups (Jiang et al., 2013). Budinova et al. (2006) deduced that basic groups could be more effectively introduced by activating in the presence of steam when compared to an inert atmosphere (N_2) . Extreme activation conditions have been shown by Lahijani et al. (2018) as detrimental to surface functional groups, with decreases in O, N and S, from 25.07 – 13.63 wt%, 1.54 – 0.34 wt% and 0.12 – 0.01 wt%, respectively, when increasing pyrolysis temperature from 500 to 900˚C. Similarly, flash carbonization has been shown to reduced O content significantly from 47.8 wt% (raw sawdust) to 24.2 wt% (air carbonized saw dust) compared to 37.0 wt% for the prepared HC (Hirst et al., 2018).

3.4. Nitrogen Containing Functional Groups

The different N-groups that can form on C-adsorbents are pyridinic, pyridonic, pyrrolic, graphitic or quaternary, amine (1˚, 2˚ and 3˚), nitro and nitroso type; aside from quaternary, all of these N-groups occur at the edge site of the graphitic plane (Saha and Kienbaum, 2019). Most N-containing groups provide basic sites with sufficient binding energies for CO_2, basic sites are often those with the lone pair of electrons in an sp^3 orbital (Adelodun et al., 2015). N content is often reported as the main factor influencing CO_2 adsorption selectivity in carbon sorbents (Wang et al., 2019). The O-atom in CO_2 presents a strong electron withdrawing property, thereby making the C-atom electrophilic, hence, when in close proximity, it binds to the electron-rich amine-nitrogen (Adelodun et al., 2015). Pyridinic-N contributes one electron to the aromatic π-system and exhibits Lewis basic characteristics (Singh et al., 2019) and can cause remarkable charge transfer to CO_2 that decreases the bond angle of CO_2 (Saha and Kienbaum, 2019). The Lewis acid-base interaction between pyridinic-N and CO_2 describes the lone pair electron donation of the N-atom to the C-atom of CO_2 (Lim et al., 2016). The *Ab initio* calculations reported by Chen *et al.* (Chen et al., 2013) demonstrated π-π interactions between CO_2 and both pyridine and pyrrolic groups. Sun et al. (2016) reported that both pyridinic- and pyrrolic-N had higher binding energies with CO_2 than quaternary-N; the interaction for the quaternary-N being dispersion interactions and pyridinic- and pyrrolic-N through electrostatic interactions. Furthermore, Ma et al. (2018) reported that the Lewis acid-base interactions between CO_2 and pyridinic-N was the strongest contributor to CO_2 adsorption with a binding energy of 21.26 kJ mol^{-1} (0.220 eV) followed by pyrrolic-N (18.60 and 10.82 kJ $mol^{—1}$ (0.193 and 0.112 eV)) and amine-N (16.45 and 5.72 kJ mol^{-1} (0.170 and 0.059 eV) which both demonstrated two configurations of CO_2 adsorption. Pyrrolic-N and amine groups facilitate both Lewis acid-base and H-bonding interactions between the N and H atoms of the group and CO_2 (Chen et al., 2012); Ma et al. (2018) reported that the H-bonding interaction was the dominant role. Pyridone-N influences CO_2 adsorption *via* exceptional H-bond interactions with CO_2 (Saha and Kienbaum, 2019), it is worth noting that pyrrolic- and pyridonic-N cannot be distinguished using XPS; therefore, they are often analysed together (Pels et al., 1995). Lim *et al.* reported binding energies for pyridone 21.61 kJ mol^{-1} (0.224 eV) and pyridine 21.03 kJ mol^{-1} (0.218 eV) that were almost twice that of alternative N-groups such as amine 14.18 kJ mol^{-1} (0.147 eV), quaternary 12.06 kJ mol^{-1} (0.125 eV), pyridine-N-oxide 11.67 kJ mol^{-1} (0.121 eV), cyanide 10.81 kJ mol^{-1} (0.112 eV) or pyrrole 10.61 kJ mol^{-1} (0.110 eV)[112].

Guo et al. (2020) reported that chemical activation of BG with H_3PO_4 or NaOH, could introduce only pyrrolic/pyridonic-N. Pyridinic-N, quaternary-N and pyridine-N-oxides were present when activating carbon using CO_2 or air, at the same temperature (850˚C,). Sevilla et al. (2011) reported results that indicated chemical oxidative treatments would introduce pyridonic-N, whereas pyrolytic treatments favour pyridinic- and quaternary-N; mild chemical treatments (KOH/precursor = 2 and T < 800˚C) will form pyridonic-N that constitute up to 10.1 wt% of the porous carbon. Remarkable decreases in N-content (10.14 to 4.05 wt%) were reported when increasing activation temperature from 600 to 650˚C due to N being more easily oxidised than C (Sevilla et al., 2011). Chen et al. (2016) identified that at a KOH to urea-modified carbon mass ratio of less than 4, pyrrolic/pyridonic-N which has been shown to be more beneficial for CO_2 adsorption (Sánchez-Sánchez et al., 2014) becomes the predominant species over pyridinic- and quaternary-N. Contrastingly, increasing KOH/Carbon ratios (0.5 to 2), when activating crab shell without any additional N doping, both quaternary-N and pyridinic-N-oxides increase while pyrrolic-N is mostly unchanged and pyridinic-N decreases (Chen et al., 2015). Heat treatments with NH_3 below 600˚C have been shown to successfully introduce pyrrolic-/pyridonic-N, pyridinic- and amino-N whilst removing O-containing functionalities (Zhang et al., 2016). -OH groups when present will react with the amino groups of urea which leads to the integration of N in the form of -NH_2, pyridinic- and pyrrolic/pyridonic-N (Chen et al., 2016) that will transform to quaternary-N at higher temperatures (Lin et al., 2012). These groups however, are lost during subsequent activations with for example KOH (Nowicki et al., 2015), or when increasing activation temperatures (Chen et al., 2015) (from 500 to 700˚C). Ma et al. (2018) reported that carbonization temperatures of 600˚C resulted in high amounts of amide groups that were transformed into protonated graphitic-N, pyridinic-N and oxidized-N species at 700˚C. Saha et al. (2017) reported that increasing activation time from 45 to 60 minutes with NH_3 will result in the decrease of graphitic-N (75 %) followed by nitro- (66.67 %) and pyrrolic/pyridonic-N (33.33 %); pyridinic-N and amino groups suffered the smallest decomposition

(c. 5 %). Combinations of high temperature NH_3 and CO_2 modifications (500 to 900˚C) can significantly improve the introduction of N moieties when compared to solely CO_2 modification (Zhang et al., 2016), reaching a maximum doping at 800˚C. N-containing functionalities can also be attained by nitration followed by reduction on the C surface (Chingombe et al., 2005). Dissociation of HNO_3 forms highly active intermediate nitronium ions that react with the aromatic rings and turn into nitrated products (-NO_2) on the carbon surface; the addition of concentrated H_2SO_4 is necessary to facilitate the formation of nitronium ions (Rajapaksha et al., 2016). Nitrogen-groups are introduced *via* electrophilic aromatic substitution, the subsequent reduction of these using sodium dithionite results in amino groups (Chingombe et al., 2005, Rajapaksha et al., 2016, Yang and Jiang, 2014). Alternative chemicals for N-doping such as $NaNH_2$ (Liu et al., 2019), acetonitrile (Wang and Yang, 2012) and NH_4OH (Aijaz et al., 2014) have also been reported.

The adsorption of CO_2 on amine-modified carbons occurs *via* multiple mechanisms, namely pore diffusion, chemical bonding, and simultaneous physisorption and chemisorption. The performance of amine-modified carbons is more apparent at elevated temperatures because the amine groups tend to block the entrance of pores and lower the surface area and micropore volume (Plaza et al., 2007). As with conventional absorption, the general consensus for the reactions of CO_2 with amine groups is the intermediate formation of a zwitterion (Zelenak et al., 2008), followed by deprotonation by the amine (a Brønsted base) (Nakao et al., 2019). However, because the shift in the electric potential of the adsorbent can create alternative adsorption sites, adsorption occurs mainly *via* physisorption, specifically, van der Waals forces (Stavitski et al., 2011). H-bonding interactions have also been identified as the major contributor in some studies (Saha and Kienbaum, 2019). Su *et al.* (Su et al., 2010) have proposed that primary and secondary amines react with CO_2 to form carbamates and tertiary amines produce bicarbonates. Furthermore, Kishor *et al.* (Kishor and Ghoshal, 2016) have reported that primary and secondary amines are more reactive towards CO_2 than tertiary amines.

3.5. Sulphur Containing Functional Groups

Compared to traditional dopants such as nitrogen, sulphur is much larger and hence protrudes out of the graphene plane thereby generating strain and defects within the framework (Saha and Kienbaum, 2019, Denis, 2013) which could give rise to charge localization that could favour the adsorption of CO_2. The effect of S-doping can also increase local reactivity due to the lone pair electron donation of the S-atom (Kiciński et al., 2014). The formation of strong acid-base interactions between CO_2 and basic C-S functionalities alongside strong pole-pole interactions due to the large quadrupole moment of CO_2 and the polar S-groups suggests the S-doping of C-based adsorbents could play a predominant role in CO_2 adsorption (Xia et al., 2012). Seema *et al.* (Seema et al., 2014) reported a linear relationship between the CO_2 capacity and quantity of oxidized-S in the S-doped porous-carbons they prepared. DFT calculations indicated that the interactions of CO_2 with sulfoxides and sulfones were stronger than those with N-moieties, such as pyrrole. The binding energy of CO_2 with pyrrole-N was 14.2 kJ mol^{-1}, which was lower than those of CO_2 with the di- (17.9 kJ mol^{-1}) or mono-oxidized (25.1 kJ mol^{-1}) S-moieties of thiophene (Chandra et al., 2012).

Generally, the synthesis of S-doped carbons can be achieved by: i) carbonization of sulphur-containing precursors (organic polymers, aromatic compounds, ionic liquids or biological substances) with subsequent activation to develop porosity; or ii) activation of porous-carbon precursors by sulphur containing agents (Saha and Kienbaum, 2019). Similar to the N-doping of porous-carbon, any subsequent activations to generate porosity will reduce the final S-content.

3.6. Interaction of CO_2 and Functional Groups in the Presence of Moisture

Even though most carbonaceous adsorbents present good stability under moist conditions, the presence of moisture within flue gas cannot be ignored given that it generally represents the third most abundant component after N_2 and CO_2. The adsorption of H_2O within the pores of carbons will depend on the surface chemistry and presence of various heteroatoms. Generally, hydrophilic carbons present an abundance of SFGs which can initiate predominant water adsorption through the hydrogen bonding between H_2O and SFGs even at relative pressures below 0.1; with respect to hydrophobic carbons with limited SFGs, H_2O adsorption typically follows the type V IUPAC classification with a large H2- hysteresis loop (Querejeta et al., 2016, González et al., 2013). The presence of SFGs and mineral matter have all been found to promote water adsorption in the low pressure range with SFGs acting as nucleating sites for H_2O to grow into clusters, while mineral impurities reduce and inhibit access to available surface area by filling or blocking porosity (Querejeta et al., 2016, Bedia et al., 2007). Competitive adsorption is influenced by both the adsorption mechanisms of pure components with various adsorption sites and the interactions between the adsorbed components both on the surfaces and in the pores of the materials (Bell et al., 2021). The availability of literature on this competitive adsorption and hence, understanding of the influence moisture may have on the adsorption of CO_2 is not comprehensive.

The presence of N-containing groups can contribute to an increased hydrophilicity which originates from the H-bonding of water and polar N-functionalities (Saha and Kienbaum, 2019). It has been reported that all N-species (bar amino groups (Wang et al., 2017 Sep, Wang et al., 2020)) suffer deterioration in the presence of moisture, especially at elevated temperatures and in the presence of larger ultramicropore volume (Saha and Kienbaum, 2019) as a result of competitive dispersion-repulsion interactions with the surface and competing electrostatic interactions (Psarras et al., 2017). Psarras *et al.* (Psarras et al., 2017) reported that when increasing the concentration of H_2O in binary CO_2/H_2O mixtures from 0 to 1 %, quaternary-N was found to be the most stable with a 13 % loss in ideal CO_2 capacity. Pyrrolic-N and pyridonic-N groups lost 25 and 28 %, respectively, whereas the pyridinic-N-oxide group lost 58 %. Increasing H_2O concentration to 10 % caused a drop in ideal CO_2 adsorption capacity of 98 % for quaternary-N and 97 % for pyridinic-N-oxide groups. Pyrrolic-N however, demonstrated the greatest stability over $0 < p/p^0 < 0.25$. Aside from the absence of O, pyrrolic-N, has a smaller Bader partial charge compared to quaternary- and pyridonic-N due to its bonding withH. Combined with the strained 5-membered ring that creates more vacancy space within the groups immediate vicinity, pyrrolic-N can be considered sterically unhindered (Psarras et al., 2017). The effect of temperature on CO_2 adsorption performance was shown to be non-linear. Whilst increasing N-content up to 28 wt% could mitigate the presence of low humidity (1 % H_2O), it was not compatible with CO_2 separation at ambient temperature and 10 % humidity. Monotonic increases in selectivity when increasing N-content, however, have been reported by Saha *et al.* (Saha et al., 2017) in their lignin-derived porous carbon activated with NH_3. In the DFT study of Xiao et al. (Xiao et al., 2014) the adsorption of CO_2 in the presence of moisture on N-substituted/grafted graphene identified a number of positive contributions as a result of either electrostatic interactions or bicarbonate formation. With regards to the N-substituted graphene, the H_2O molecule can weakly bond to the N-site with an energy of -3.6 kJ mol^{-1}, this water molecule can then adsorb CO_2 through a C-O_{water} electrostatic interaction with an adsorption energy of -14.1 kJ mol^{-1}. Alternatively, CO_2 can interact with H_2O to form bicarbonate which is further bonded to the N-site; the OH-N bond distance being 1.5 Å suggesting a strong hydrogen bond, the adsorption energy for this configuration being -54.5 kJ mol^{-1}. When grafted with an -NH_2 group, CO_2 can be adsorbed through two configurations. The first is the adsorption of CO_2 over an -NH_2 site to form a carbamate, this is then stabilised by H_2O with two H-O bond distances of 1.8 Å, the total adsorption en-

ergy calculated as -42.3 kJ mol^{-1}. Alternatively, CO_2 and H_2O may form bicarbonate which can be adsorbed on -NH_2 groups through hydrogen bonding with an H-N bond distance of 1.5 Å, with an adsorption energy of -57.6 kJ mol^{-1}. The effect of -NH_2 density was also evaluated. Here, the presence of a second -NH_2 group was shown to weaken the adsorption energy to -50.7 kJ mol^{-1} as a result of the repulsive force between neighbouring N and =O in the formed bicarbonate (Xiao et al., 2014). Pokrzywinski et al. when studying the effect of moisture on milk-derived microporous carbons identified that under a stream of humidified-CO_2 the adsorption behaviour of the carbon was not impacted by the presence of H_2O since its kinetic behaviour favoured CO_2 saturation first (Pokrzywinski et al., 2020). This observation was not apparent when evaluating the adsorption under humid-simulated flue gas. In this case, the presence of N_2 was postulated to decrease the adsorption kinetics of CO_2 and hence, increase the likelihood of H_2O co-adsorption.

4. Surface Modification for Increasing Effective Functional Groups

4.1. Heat Treatments

Typically, the thermal treatment of carbon materials generates more basic surface functional groups *via* the removal of hydrophilic groups, such as carbonyl and ether (Ahmed et al., 2016). During the thermal treatment of biochar in the temperature range of 800–900°C for up to 2 h, gases such as H_2, air, or Ar can be introduced to enhance the formation of additional functional groups on the biochar surface (Li et al., 2014). Shen *et al.* (Shen et al., 2012) demonstrated that H_2 can stabilize the surface of carbons by deactivating sites *via* the formation of stable C–H_x bonds, which simultaneously increases the surface basicity . Most oxygen SFGs can be removed *via* decomposition at temperatures in the range of 800–1000°C (Figueiredo et al., 1999). The heat treatment temperature is limited to approximately 1000°C, which produces materials with a low reactivity for O_2 or chemical agents and a high degree of basicity (Shafeeyan et al., 2010). The high basicity of these materials is attributed to the O-free *Lewis basic* sites on the graphene layers and residual O-containing SFGs (*e.g.*, pyrone and chromene) (Shafeeyan et al., 2010, Papirer et al., 1987, Dandekar et al., 1998). Guo et al. (2020) used several chemicals and gases, including H_3PO_4, NaOH, CO_2, and air, to modify sugarcane bagasse (BG) waste . The CO_2 or air thermal treatments were performed at 850°C for 2 h after an initial pyrolysis step at 750°C for 1 h under an N_2 atmosphere. The air-modified sample presented an extremely low (Brunauer-Emmett-Teller (BET)) surface area of 99 m^2 g^{-1} but myriad oxygen and nitrogen-containing SFGs. These groups include pyridinic, pyrrolic/pyridonic, quaternary and pyridine-N-oxides (total surface N concentration = 2.46 at%) alongside ketones, carbonyls, lactone groups, ethers, alcohol and carboxyl groups (total surface O concentration = 30.55 at%). In contrast, Xu et al. (2016) synthesized waste-derived alkaline biochar by heating sewage sludge, pig manure and wheat straw at a low temperature of 500°C (a ramp rate of 10°C min^{-1} for 4 h). CO_2 was adsorbed onto the obtained biochar samples *via* both physisorption and chemisorption depending on the adsorption temperature. Lahijani et al. (2018) investigated metal-impregnated biochars obtained *via* the single-step pyrolysis of walnut shells at 500, 700, and 900°C. The biochar produced at 900°C presented the highest specific surface area and micropore volume of 397 m^2 g^{-1} and 0.16 cm^3 g^{-1}, respectively, among all the prepared samples. Moreover, it was reported that the adsorption capacity of the biochars increased from 0.63 to 1.57 mmol g^{-1} as the activation temperature increased from 500 to 900°C, respectively, owing to the structural changes that biochar underwent during treatment. Furthermore, the number of surface functionalities decreased with increasing temperature. At 900°C the number of SFGs on the biochar surface was negligible, which indicated that physisorption was the governing mechanism.

Creamer *et al.* (Creamer et al., 2014) produced biochar *via* the slow pyrolysis of BG and hickory wood (HW) at 300, 450, and 600°C under an N_2 atmosphere (BG300, BG450, BG600, HW300, HW450, and HW600, respectively). As expected, the samples produced at higher temperatures boasted a higher level of porosity, specifically micropores (Lehmann and Joseph, 2012). Moreover, BG450 and HW450 presented the highest and lowest C and O contents, respectively, among all of the samples. Alkane and cyclic alkene groups were present on the surface of BG300 and BG450, and the Fourier-transform infrared (FTIR) spectra of these samples also revealed the presence of either S-, amine, or ester groups on their surfaces. The presence of cyclic alkene groups on the surfaces of HW300 and HW450 was also reported. Several of these groups were absent on the surfaces of BG600 and HW600; however, the number of N-containing groups on the surfaces of these samples was higher than that on the surfaces of the samples prepared at lower temperatures. It has been observed that high temperatures can induce dehydration and deoxygenation reactions that reduce the number of both H- and O-containing SFGs (Guo and Rockstraw, 2007, Mukherjee et al., 2011, Ahmad et al., 2014). In addition to the surface area being a determining factor in the adsorption of CO_2, the presence of N-containing groups also played an important role when sufficient surface area was accessible (Creamer et al., 2014) (Figure 4).

Hirst *et al.* (Hirst et al., 2018) investigated non-homogenous sawdust from the residues of eucalyptus wood that were heated to 400°C (a ramp rate of 10°C min^{-1}) under N_2 flow, followed by switching the gas to air and holding at 400°C for 5 – 10 min. This led to an increase in the C-content from 46.4 to 72.4 wt% and a decrease in the H- and O-contents from 5.8 to 3.2 wt% and from 47.8 to 24.2 wt%, respectively. In addition, this study demonstrated that air-carbonized carbon materials were resistant to KOH activation, and consequently, retained a high fraction of microporosity even under severe activation conditions. The adsorption capacity of these materials was as high as 5 mmol g^{-1} at 1 bar and 25°C, owing to the size of most pore channels being approximately 0.8 nm. A summary of the heat treatment methods discussed in this section is given in table S1 in the supplementary information. The author is advised to treat this table as an indication of what these methods can result in and not a recipe for SFG introduction. Comprehensive descriptions of employed methods are rarely given and even if they were, the importance of precursor, pre-treatments as well as the presence of impurities is extremely influential in the final carbonaceous adsorbent.

4.2. Acidic Treatments

Jiang *et al.* (Jiang et al., 2013) successfully introduced both –OH and –COOH groups on the surface of HNO_3-activated red cedar wood biochar; x-ray photoelectron spectroscopy (XPS) data calibrated by the C 1s signal at 284.6 eV revealed the total surface coverage of these O-SFGs to be around 15%. These O-containing surface complexes presented electron-rich properties; therefore, the introduction of both –OH and –COOH groups can enhance the interactions between CO_2 and porous carbons. Furthermore, Masoudi Soltani *et al.* (Salman et al., 2014) used HNO_3 for the surface modification of pyrolyzed cigarette filters using different HNO_3 concentration and contact times and conducted a full factorial experiment to investigate the effects of the modifications on the surface area of the synthesized porous carbons. They reported that HNO_3 could increase surface acidity by 57.8% to 1.21 mmol g^{-1} and the O-content by a factor of approximately 2.5. Lactonic, –COOH, and phenolic groups were present on the surface of the prepared carbon. Budinova *et al.* (Budinova et al., 2006) evaluated H_3PO_4 impregnation on the subsequent activation of biomass by subjecting H_3PO_4-treated biomass to (1) pyrolysis at 600°C (a ramp rate of 3°C min^{-1}) for 1 h under an N_2 atmosphere, (2) the same as in (1) followed by activation at 700°C (ramp rate of 3°C min^{-1}) for 1 h in the presence of steam, and (3) heating to 700°C (ramp rate of 3°C min^{-1}) in the presence of steam for 2 h. The chemically-modified sample obtained using method (1) presented the highest content of –COOH groups (0.744 meq g^{-1}), whereas the sample prepared using method (2) presented high contents of both –OH (0.572 meq g^{-1}) and carbonyl groups (2.530 meq g^{-1}). In

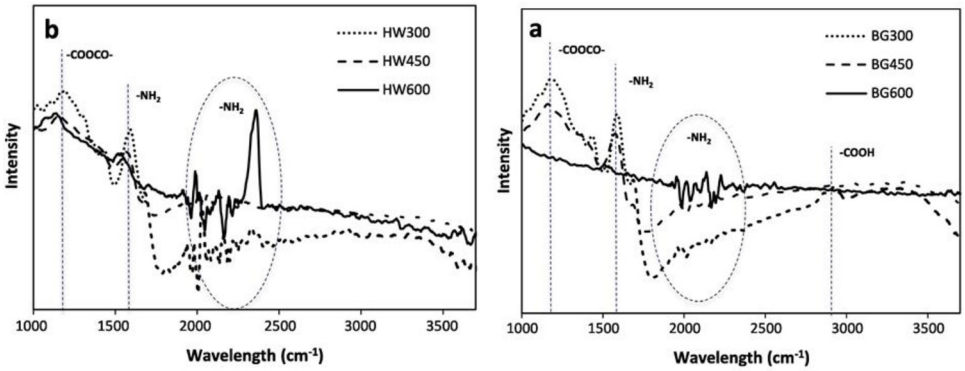

Figure 4. FTIR spectra of the biochar samples prepared at different temperatures: a. sugarcane bagasse; b. hickory wood. Reproduced from (Creamer et al., 2014).

addition, the carbon prepared using method (1) presented the lowest pH (4.5), which was consistent with its content of –COOH groups, lactones, lactoles, and P-containing acidic groups. The carbon material obtained using method (2) presented the highest content of basic groups, and the carbon material obtained using method (3) presented the highest pH (6.5), which was consistent with its –COOH group content being the lowest. Food wastes can also be used as carbon precursors, Opatokun *et al.* (Opatokun et al., 2017) pyrolyzed fresh food waste to produce char. The CO_2 activation process was performed at 900°C for 1.5 – 2 h, and 69% HNO_3 was used for 1 h oxidation at 60°C at a 1:10 ratio (activated char:HNO_3). Melamine amination involved stirring 2 g of activated biochar for 5 h at 70°C in a melamine suspension (1.3 g melamine in 100 mL of 80% ethanol), followed by carbonization at 450°C for 50 min. The capacity difference between the unanimated (4.41 mmol g^{-1}) and animated sorbents (4.36 mmol g^{-1}) at 25°C and 1 bar was negligible. The negligible difference in CO_2 adsorption capacity is a result of adsorption performance being heavily dependent on a combination of micropore volume, pore size and nitrogen content; the scale of their influence depending on the adsorption conditions such as CO_2 partial pressure (Petrovic et al., 2020).

Singh et al. (2018) subjected biomass to acid-assisted polymerization and solid-state activation to produce functionalized porous carbons. Hydrothermal carbonisation was used for biomass waste upcycling, wherein biomass was first subjected to high-pressure heat treatment before activation. This facilitated the formation of different intermediates and resulted in the development of an aromatic network with high C content and numerous O functionalities (Alatalo et al., 2016, Regmi et al., 2012, Liu et al., 2015). Singh *et al.* (Singh et al., 2018) proposed that acid treatment prior to KOH activation could be used as an alternative to high-pressure treatment to obtain cross-linked carbons, introduce O-containing functional groups *via* oxidation and dehydration, and dissolve the inherent inorganic metallic constituents within the biomass. The acid treatment involved mixing the powdered biomass (5 g) with milli-Q water (10 mL) and H_2SO_4 (2.24 mL) for 6 h in an air oven at 100°C followed by heating at 160°C for 6 h. Subsequently, the product underwent solid-state activation with KOH at 600°C and at different impregnation ratios. FTIR spectra revealed the high aromaticity of the carbons and presence of O-SFGs, such as phenolic and carboxylic acids, which imparted negative charge to the surface and could therefore enhance the adsorption of CO_2. H_2SO_4 presented a strong dehydrating effect, removed most of the inorganic impurities, and was demonstrated to catalyse the polymerization of carbons prior to activation. The O-content of the prepared carbons as determined from XPS, ranging between 11.2 and 43.5 %, was ascribed to the presence of phenolic, carbonyl, and ether groups in the sample, and facilitated a CO_2 adsorption capacity of 3.2 mmol g^{-1} at 25°C and 1 bar. The observed CO_2 adsorption capacities were higher than those reported in a previous study, in which the acid pre-treatment was omitted (Regmi et al., 2012). This was attributed to the development of O-functionalities *via* polymerization and removal of impurities, such as sylvite, which induced a change in the surface charge of the adsorbent.

Zhang et al. (2015) evaluated the effects of de-ashing rice husk prior to NH_3 modification. The deashing procedure involved mixing HF (20 mL, 40%), deionized water (60 mL), and raw rice husk (25 g) for 24 h at 60°C. The pre-treatment facilitated pore development during ammonification, as there are more opportunities for free radicals to pass through (Lua et al., 2006). In addition, the pretreatment promoted the introduction of N-SFGs, likely owing to the increased availability of active sites, which has also been reported by Shafeeyan *et al.* (Shafeeyan et al., 2011). The removal of the Si-rich structure promoted the development of the porous structure and introduction of N-SFGs, and also increased the surface activity which enhanced both physisorption and chemisorption (Shen and Fan, 2013). Sodium alginate can also be used to introduce different O-containing groups, such as –COO and –OH, which are bonded to the edges of C-atoms prior to NH_3 modification (Hosseini et al., 2017). Hosseini et al. (2017) demonstrated this by enriching the N-content of gel beads derived from an eggshell composite calcined at 1000°C (1273 K) for 4 h using sodium alginate. A summary of the acidic treatments discussed in this section is given in table S2 of the supplementary information; as with table S1, the author is advised to exercise precaution on interpretation.

4.3. Basic Treatments

Alabadi *et al.* (Alabadi et al., 2015) prepared a number of porous carbons from gelatine and starch biomass *via* dry chemical activation. Different carbonized gelatine- and starch-to-KOH mass ratios were used, and chemical activation was followed by heating at 700°C at a heating rate of 10°C min^{-1} under an N_2 atmosphere for 10 min. Activation led to the formation of –OH and $–NH_2$ groups on the carbon surface next to other O-functionalities in non-conjugated and conjugated systems (Diez et al., 2012). Nitrogen contents up to 3 at% were achieved in the form of pyridinic, pyrrolic and pyridone groups, with pyridine groups being prevalent in the sample comprised of equal parts (1:1, w/w) parts of gelatine and starch. This sample presented the highest adsorption capacity (3.84 mmol g^{-1} at 25°C and 1 bar), which was ascribed to the combination of high micropore volume (Sevilla et al., 2013), amount of residual –OH groups, and ratio of non-C elements, such as N and O, retained in the activated carbons (ACs) (Alabadi et al., 2015).

Chen et al. (2016) used a combination of urea and KOH to synthesize porous carbon from coconut shell, and reported that the N-doping occurred prior to activation. Pre-modification involved mixing the carbonized shell with an equal amount of urea followed by heating in air to 350°C for 2 h. The N-content was seen to increase up to 4.47 wt% *via* reactions between urea and the adsorbent's existing SFGs, followed by thermal conversions which included the reactions between the -OH and $-NH_2$ amino groups. The N-groups consisted of pyridinic (32.6 – 51.9 at%), pyrrole/pyridine (32.6 – 52.8 at%) and quaternary-N (11.7 – 20.4 at%) groups. Pyridine-type N-groups have been frequently reported as the most influential in enhancing CO_2 adsorption (Sánchez-Sánchez et al., 2014). Chen et al. (2015) prepared a series of adsorbents and demonstrated that crab shell was a promising precursor for N-rich

ACs. The carbonization and KOH activation of crab shells resulted in an N-content in the range of 5.1-8.5 wt% in the form of quaternary (11.7 – 20.1 at%), pyrrolic (45.1 – 47.3 at%), pyridinic (25.6 – 35.1 at%) and pyridinic-N-oxides, with pyrrolic nitrogen being the predominant form which facilitated a CO_2 adsorption capacity of 4.37 mmol g^{-1} at 25°C and 1 bar. This capacity was ascribed to micropore filling and N-SFGs that contributed up to 78.2 % of the adsorption of CO_2 on the prepared samples with less-developed porosity. The contribution decreased to below 15 % for well-developed microporous structures. Nitrogen-enriched microporous carbons were produced from coffee grounds *via* KOH activation (Wang et al., 2020). After carbonization at 600°C) for 4 h at heating rate of 5°C min^{-1}, the biochar was mixed with KOH at various ratios and activated at 800°C. The N-content was increased up to 0.74 at% with pyrrolic-N (44.30 at%) being the predominant species, followed by graphitic- (29.14 at%) and pyridinic-N (26.56 at%). Pyrrolic and pyridinic-N effectively ameliorated the polarity of carbon and facilitated the adsorption of CO_2 (Peng et al., 2019) and pyridinic-N presented the predominate contribution (Peng et al., 2019).

Alternative activating agents such as K_2CO_3 have also been demonstrated to be effective for the synthesis of porous N-doped carbons. Yue *et al.* (Yue et al., 2018) successfully adopted this approach with coconut shells. Nitrogen was doped into the carbon framework using urea prior to activation, and the sample exhibited a CO_2 adsorption capacity of up to 3.71 mmol g^{-1} at 25°C and 1 bar. The development of pores can be hindered by some inorganic species present in different biomass wastes, such as fruit stones and shells, blocking pore entrances. Li and Xiao (2019) reported a CO_2 activation method followed by K_2CO_3-promoted leaching using rice husk ash. The former was intended to develop an initial porosity and the latter to promote the leaching of inorganic silica. The obtained carbon presented both micropores and mesopores and its CO_2 adsorption capacity reached 3.1 mmol g^{-1} at 25°C and 1 bar.

4.4. Amination and Ammoxidation

When carbons are activated with NH_3 at high temperatures, nitrogenous groups are typically introduced and acidic O-groups are mostly removed (Shafeeyan et al., 2010). The N-groups formed *via* reactions with NH_3, HNO_3, and amines can include $–NH_2$, imide, pyrrole, pyridine, and lactam (Plaza et al., 2009, Pevida et al., 2008). Jansen and Bekkum (Jansen and van Bekkum, 1994, Jansen and van Bekkum, 1995) demonstrated that the adsorbent modification method will determine the specific N-species introduced on the surface. Ammoxidation leads to the development of amides, whereas amination favours the formation of lactams and imides. Subsequent heat treatment leads to the transformation of these groups into pyridinic and pyrrolic species. The presence of O-SFGs can also play an important role in increasing the efficiency of N-incorporation (Petrovic et al., 2020). Therefore, the pre-oxidation of carbonaceous materials can enhance subsequent N-doping treatments (Shafeeyan et al., 2011). When these O-groups decompose during NH_3 treatment, the reactivity of N-containing free radicals increases and hence, further promotes the development of basic groups, such as amide and pyridine species. The order of modification methods can also affect the amount of N that can be introduced into carbons. Pietrzak (Pietrzak, 2009) reported that the introduction of N into carbons *via* ammoxidation after activation decreased pore volume and surface area, and consequently, capacity under their experimental conditions, owing to the pore blockage effect. Furthermore, they demonstrated that the introduced N-species, namely imines, amines, amides, pyrrolic/pyridonic-, and pyridinic-N, could be formed regardless of the procedure.

Zhang et al. (2016) employed a combination of KOH activation and ammonia modification when synthesising porous carbon from black locust waste biomass with a view to incorporate nitrogen functionalities during carbonisation. The three-step procedure involved an initial carbonization at 650°C, KOH activation at 830°C and ammonia modification at 600°C. Both activation and surface modification occurred during the NH_3 modification step, which increased the development of pores, and subsequently decreased the BET surface area (from 2511 to 2064 m^2 g^{-1}) and total pore volume (from 1.35 to 0.98 cm^3 g^{-1}). This was attributed to the thermal decomposition of the surface O-groups that might have been blocking micropore entrances or filling micropores, and therefore, might have been creating vacant sites (Shafeeyan et al., 2011, Pevida et al., 2008). The free radicals present during ammonification (NH_2, NH, and H) could subsequently react with the vacant sites to expand the pore structure at high temperatures, according to the following equations Eq. 1 to Eq. 3 (Shafeeyan et al., 2010, Laheäär et al., 2014, Yuan et al., 2020):

$$R - COO - NH_4^+ - H_2O \rightarrow R - CO - NH_2 - H_2O \rightarrow R - C \equiv N \quad (1)$$

$$R - OH + NH_3 \rightarrow R - NH_2 + H_2O \quad (2)$$

$$R - C = O + NH_3 \rightarrow R - C = NH + H_2O \quad (3)$$

The reactions between the free radicals and the mesopore walls of the carbon will lead to the release of gaseous H_2, CH_4, HCN, and cyanogen, which could further develop new micropores *via* secondary *in-situ* activation (Shafeeyan et al., 2010, Laheäär et al., 2014). In addition to textural enhancements, NH_3 treatments increase the N-content of porous carbons. Zhang *et al.* (Zhang et al., 2016) reported an increase of up to 7.21 wt% accompanied by a decrease in O-content from 24.49 to 14.93 wt%, which confirmed the aforementioned hypothesis. Ammonia reacts with carboxylic acid sites to form ammonium salts, which lead to the formation of amides and nitriles *via* dehydration or the substitution of –OH groups by the amides on the carbon surface (Laheäär et al., 2014). In this study, the N in the carbon matrix was present as pyrrolic/pyridonic, pyridine, and amino-type N-groups, such as amide, imine, and amine (Xing et al., 2012). The combination of basic groups and textural properties led to a CO_2 adsorption capacity of 5.05 mmol g^{-1} at 25°C and 1 bar and a CO_2 selectivity over N_2 of 30.75 at 25°C as calculated using the ideal adsorbed solution theory (IAST). The adsorption was demonstrated to be both physical and chemical, as validated by the elevated isosteric heat of adsorption (Q_{st}) values. This modification method was an effective way of producing highly ultra-microporous sorbents that could adsorb CO_2 both physically and chemically; moreover, it presented high selectivity, fast kinetics, and good cyclability.

Nguyen and Lee (2016) produced N-doped biochar beads from chicken manure. The procedure involved drying and subsequently pyrolyzing the waste at 450°C for 1 h followed by mixing the product with a HNO_3 solution (15.7 N) at a 1:10 solid-to-liquid mass ratio. Thereafter, the product was separated from the aqueous phase and treated with anhydrous NH_3 gas for 1 h at 450°C. Ammoxidation can generate active alkaline sites that can introduce N-containing functional groups *via* oxidation reactions with HNO_3 and NH_3 (Deng and Ting, 2005, Nowicki et al., 2009). Nguyen *et al.* (Nguyen and Lee, 2016) achieved N-contents of up to 6.32 wt%; moreover, the C- and H-contents of the prepared porous carbon increased as confirmed by combustion elemental analysis, whereas the O-content decreased.

N-rich agricultural waste soybean straw has been demonstrated as a promising precursor for porous carbons. Zhang et al. (2016) prepared a series of sorbents which were then modified with CO_2, NH_3 and CO_2–NH_3 in the temperature range of 500–900°C at a hold time of 0.5 h . At high temperatures, the CO_2–NH_3 mixture produced the greatest number of free radicals, which could participate in gas–solid reactions. The highest N-doping was achieved at 800°C, and approximately 6 wt% N was successfully doped into the modified biochar *via* NH_3 and CO_2–NH_3 treatments. The CO_2–NH_3 mixture produced higher N-contents and N-to-C ratios than NH_3 alone, which indicated that the presence of CO_2 in the gaseous activating medium promoted the introduction of N-groups. That was attributed to the reactions between carbon and CO_2, which provided more active sites for amination (Shafeeyan et al.,

2011). The combination of CO_2 activation and high-temperature amination improved both the microporosity and N-doping levels of the porous carbon. A summary of the basic treatments discussed in this section is given in table S3 of the supplementary information; as with table S1 and S2, the author is advised to exercise precaution on interpretation.

4.5. Amine Modification

Generally, carbons are, comparatively, less advantageous than some other class of adsorbents such as zeolites with respect to their adsorption capacity and selectivity at low CO_2 partial pressures, which are specific to many large anthropogenic point sources. These shortcomings can be addressed by introducing $–NH_2$ functionalities into the carbon frameworks (Arenillas et al., 2005, Dindi et al., 2017). The presence of $–NH_2$ functionalities can significantly improve the CO_2 adsorption capacity of carbons, which becomes even more influential at low CO_2 concentrations. When amino groups are immobilised, they can react with CO_2 to produce carbamates *via* the formation of zwitterionic intermediates. This is similar to the absorption of CO_2 using primary alkanolamines (Samanta et al., 2012). The reaction pathways favour the formation of carbamate and bicarbonate at low temperatures, whereas at elevated temperatures, the equilibrium was observed to shift and dissociation into amine and CO_2 was favoured (Harlick and Sayari, 2006). Three major amine immobilization pathways are known, *i.e.* physical impregnation of supports with amines, covalent bonding of amines to supports, and *in situ* polymerization of amine-containing precursors (Sarmah et al., 2013, Fashi et al., 2020).

The wet impregnation method of introducing amine compounds into AC has been extensively reported in the literature (Rashidi and Yusup, 2016). This process typically involves mixing the aqueous amine solution and carbons under specific temperature and agitation conditions. Houshmand *et al.* (Houshmand et al., 2011) reported that amines are dispersed within the adsorbent pores and also on the internal and external surfaces of the carbons during impregnation. Furthermore, amines are physically adsorbed *via* dipole-dipole interactions, *van der* Waals forces, H-bonds, acid-base interactions, and ion-exchange reactions. The main drawbacks of amine-modified solids are the possible loss of NH_3 at the regeneration temperature (Franchi et al., 2005) and the intensity of the regeneration process (Hao et al., 2010), which requires high temperatures, similar to those of conventional amine-based absorption processes.

Wang et al. (2017 Sep) evaluated the effects of tetraethylenepentamine (TEPA) monoethanolamine (MEA), diethanolamine (DEA), polyethyleneimine (PE), and diethylenetriamine (DETA) on a selection of waste wood ashes (WA), which were introduced *via* wet impregnation of the supports. The procedure consisted of dissolving a specific quantity of amine in deionized water (50 mL) followed by the addition of ash (10 g) under stirring at ambient temperature for 10 h and subsequent drying and calcining at 130°C for 4 h. After TEPA and WA-1 were determined to be the most suitable amine and support, respectively, the support was loaded with 15 – 75 wt% of TEPA. TEPA was selected because it presented the greatest regeneration capability and conversion; however, the efficiency of the TEPA-modified WA 1 support was lower than that of its DEA-modified counterpart. As the TEPA loading increased, the amine became more evenly distributed; however, at the high loadings of 60 and 75 wt%, the amine particles began to aggregate into large blocks. This blocked the pores hence, reducing the surface area of the carbons; therefore, excessive amine loading led to a decrease in the number of available active sites (Zhang et al., 2014, Zhang et al., 2014).

Alternatively, it is possible to chemically anchor the amino groups to the surface of the adsorbent through grafting. Given the dependence of physical adsorption on pore size and volume, Houshmand et al. sought to improve the specific interaction of a microporous AC and CO_2 by grafting a halogenated amine (2-chloroethylamine hydrochloride, CEA) on the oxidised surface (Houshmand et al., 2013). Using a two-stage modification, the palm shell derived AC was first oxidised with nitric acid (8 N), and then treated with NaOH solution (1 M) under stirring for 24 hours. The sample was then washed, dried and subsequently treated with CEA solution (1 M) in a shaker for 24 hours. By oxidising with nitric acid, halogenated amines can react with the hydroxyl within the carboxylic/phenolic group, hence with the alcoholic groups themselves (Houshmand et al., 2011). By comparing the nitrogen and volatile contents of the grafted samples and their associated decreases in surface area and pore volume, the anchoring of the halogenated amine can be inferred. By comparing CO_2 adsorption performance of the pristine, oxidised and aminated samples, the impact of these introduced functional groups can be determined. At low temperatures, the presence of these nitrogen groups was found to retard the CO_2 uptake; however, by studying the temperature dependence of CO_2 adsorption by increasing adsorption temperature by 1°C min^{-1} from 30 to 120°C, a 45 % increase in capacity was observed (>100°C) compared to the pristine AC. When normalising capacities to BET surface area to account for the reduction in such when anchoring amine groups, the grafted sample presented two and six-fold increases in capacity with the parent sample at 30 and 115°C. In the context of aliphatic or aromatic amine compounds, which can form a “bridge” when chemically bonded to substrates due to the transformation of primary amine groups to secondary during modification, Hu et al. sought to exploit the excellent CO_2 adsorption properties exhibited by their solutions and avoid the bridge-forming tendency by grafting p-phenylenediamine (PDA) to multi-walled carbon nanotubes (MWCNT)s (Hu et al., 2017). The authors postulated that the steric hinderance effect of the benzene ring would make it difficult for both of the amino groups of PDA to connect to the carboxyl groups of the oxidised carbon nanotube *via* amide bond formation; the primary amine group may remain. By first oxidising the nanotubes with mixed acids (H_2SO_4 and HNO_3), the carboxylated MWCNTs were then activated by *N,N,N,N*-tetramethyluronium hexafluorophosphate and then functionalised with PDA in a dimethyl fumarate (DMF) solution. The introduction of both primary and secondary amine groups, improves the CO_2 adsorption performance through carbamate formation (Lee and Park, 2015), electrostatic interactions due to the high electronegativity and hydrogen bonding; the excess of electrons trapped around defect sites confirmed by Raman spectroscopy and high-resolution transmission electron microscopy (HRTEM) produces localised lowest unoccupied molecular orbitals in the carbon lattice which may further improve interactions between the carbon nanotubes and CO_2 (Tachikawa and Kawabata, 2009). Using isosteric heats of adsorption, the authors observed an increase in CO_2 affinity with CO_2 loading on the PDA-grafted nanotubes, converse to the pristine materials, with increases in capacity of 100, 144 and 182 % in equilibrium capacity at 0, 5 and 10°C, respectively. The employment of diazonium chemistry has also been exploited when grafting amine groups by Grondein and Bélanger (Grondein and Bélanger, 2011). In this work, Vulcan XC72R was modified by reaction with the diazonium cations of paraphenylenediamine, 4-aminobenzylamine and 4-aminoethylaniline. The method follows dispersion of the carbon powder in deionised water, to which 0.1 eq of the diamine was introduced followed by 0.1 eq of solid sodium nitrite and finally concentrated HCl. After overnight stirring and filtration, the powder was washed with water, DMF, MeOH and acetone. The modification presents *in situ* formation of the diazonium cation from the corresponding amine followed by reduction by the carbon without isolation and is represented in Figure 5 (Grondein and Bélanger, 2011).

Typically, the properties of carbons and zeolites used as amine-loaded CO_2 adsorbents are inferior to those of mesoporous silica owing to their pore volumes and sizes being smaller than those of mesoporous silica (Chen et al., 2014). Because carbons can adsorb significant amounts of CO_2 *via* physisorption, the benefit of incorporating amine groups may not compensate their performance to overcome the decrease in surface area or pore volume. In contrast, when amine moieties are present, the adsorption can be manipulated to occur *via* both chemical and physical mechanisms, which enhances the selectivity of the adsor-

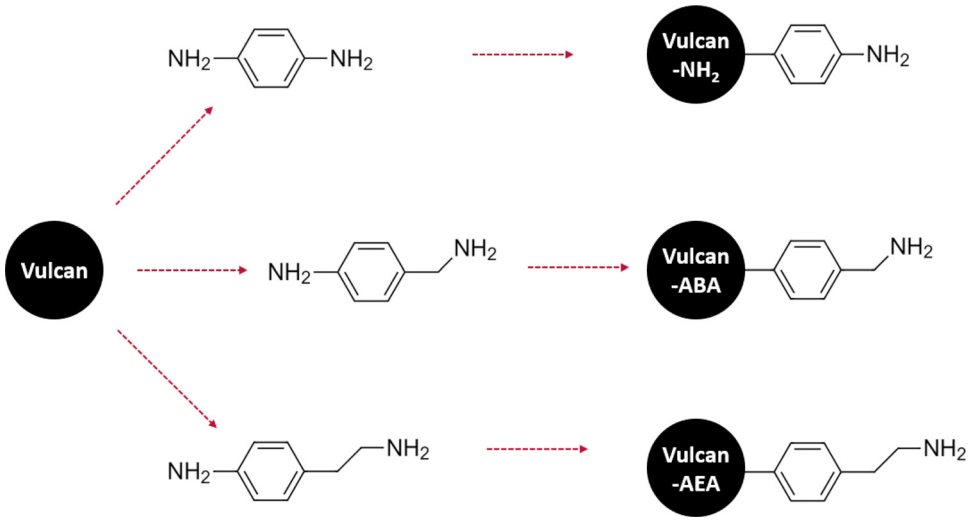

Figure 5. Modification of carbon Vulcan XC72R by in situ generated diazonium cations of paraphenylenediamine, 4-aminobenzylamine and 4-aminoethylaniline reproduced from Grondein and Bélanger (Grondein and Bélanger, 2011).

bent and performance of the C-based supports at high temperatures or under moist conditions.

4.6. Metal Doping

The impregnation of porous carbons with basic metals or their oxides can improve surface chemistry and adsorptive performance during post-combustion CO_2 capture (Chiang and Juang, 2017). Metal oxides, hydroxides, and oxyhydroxides used to impregnate porous carbons enhance the CO_2 capture performance of the supports by increasing their basicity and surface area and promoting the production of carbonates (Han et al., 2012, Pierre-Louis et al., 2013). Lahijani *et al.* (Lahijani et al., 2018) investigated the incorporation of metals into biochar for CO_2 capture under ambient conditions. They subjected walnut shells to single-step pyrolysis at different temperatures in the range of 500–900°C for 1.5 h. The biochar with the highest surface area and microporosity was subsequently impregnated with different metals (*i.e.* Mg, Al, Fe, Ni, Ca, or Na), followed by heat treatment at 500°C under an N_2 atmosphere for 15 min to oxidize the impregnated metals. Metal nitrile salt solutions (5 wt%) obtained by dissolving nitrile salts in distilled water (80 mL) were used for the wet impregnation of the metals. Biochar (1 g) was subsequently added to each solution, and the mixtures were stirred for 12 h. The CO_2 adsorption capacities of the prepared samples decreased as follows: Mg > Al > Fe > Ni > Ca > raw-biochar > Na. The Mg-loaded sorbent was prepared using magnesium nitrate hexahydrate ($Mg(NO_3)_2$•$6H_2O$), which underwent endothermic dehydration to anhydrous $Mg(NO_3)_2$ at approximately 110–190°C. Anhydrous $Mg(NO_3)_2$ decomposes to MgO at temperatures above 400°C. The formation of basic MgO sites favoured the adsorption of CO_2 *via* interactions with the basic O^{2-} ions of the O^{2-}–Mg^{2+} bonds, which facilitated the formation of carbonates (Shahkarami et al., 2016, Liu et al., 2013). Hosseini *et al.* (Hosseini et al., 2015) reported the impregnation of HNO_3-modified carbons with Cu and Zn. HNO_3 modification was used to increase the number of O-containing surface functionalities to facilitate the deposition of metals. Metal impregnation at different Cu/Zn ratios (4 – 20 wt%) was intended to produce superior sorbents. HNO_3-treated carbons were impregnated with $Cu(NO_3)_2$ and $ZnSO_4$ *via* an aqueous ion-exchange and was described as the replacement of two H^+ ions from the carbon surface with a Cu^{2+} ion (Abdedayem et al., 2015), which decreased surface acidity. The oxygen groups were found to be highly favourable to link with the metal ions to form metal complexes with the negatively charged acidic groups (Hosseini et al., 2015). This led to the negatively-charged groups on the surfaces of carbon and Cu-loaded carbon samples being surrounded by Zn^{2+} ions, which were adsorbed on the substrate surface, and consequently, facilitated surface diffusion and the reduction of ions at more favourable sites (Hosseini et al., 2015) (Figure 6).

Cobalt has also featured in surface modification of carbonaceous adsorbents, Vieillard et al. combined both aminosilane grafting and cobalt particle dispersion within cocoa shell-derived hydrochar (HC) (Vieillard et al., 2018). The authors sought to exploit the improved stability and adsorption capacity of (3-aminopropyl(triethoxysilane) (APTES) grafted sorbents whilst elucidating the role of metal nanoparticles (MNPs) in CO_2 adsorption. The authors postulated that by inducing weaker interactions between the sorbent and CO_2, the potential for fully-reversible CO_2 capture could be realised. Through promotion of CO_2, physical condensation around Co particles entrapped in compacted organic entanglement by hydroxyl and amino groups, direct contact between CO_2 and the SFGs can be avoided (Vieillard et al., 2018). Grafting the HC surface with APTES (0.3 wt%) was performed in a water-ethanol mixture (1:3 V/V) at 80°C for 6 h. The resulting sample was then treated with cobalt nitrate hexahydrate ($Co(NO_3)_2$•$6H_2O$) as a precursor and tetraoctylammonium bromide (TOAB) as a reducing agent (weight ratio: Co $(NO_3)_2$/TOAB (0.3:0.03)) in toluene for 5 h under stirring at room temperature. When studying the CO_2 adsorption of the HC, APTES-grafted HC (HC-APTES) and cobalt-modified HC-APTES (HC-APTES-Co), an increase in equilibrium capacity was observed alongside significant modification to the adsorption kinetics as depicted in Figure 7.

Of all three curves, there is a clear knee in the uptake care at around 1min which can be described when considering the kinetic-determining steps. The two steps illustrate the initial interparticle diffusion and successive intraparticle diffusion processes; in the case of HC-APTES-Co, the attenuation of the two steps is most likely a result of structure compaction after Co-incorporation reducing the contribution of intraparticle diffusion (Vieillard et al., 2018). With capacities increasing from 0.66 mmol g^{-1} (HC) to 0.92 mmol g^{-1} (HC-APTES) and 1.35 mmol g^{-1} (HC-APTES-Co), it can be deduced that both APTES-grafting and Co-incorporation, positively contribute to improving surface affinity to CO_2. The APTES influence is expected given the basicity enhancements; however, given the basicity reductions when incorporating Co (due to Co:NH_2 interactions), the authors suggested a predominantly physical and non-stoichiometric condensation of CO_2 through much weaker interaction with the Co particles entrapped in organic entanglement. The mixture of terminal hydroxyl groups and compacted entanglement which immobilises Co nanoparticles surrounded by amino groups is responsible for significant affinity enhancements as a result of the reduction in surface basicity; this reduction to surface basicity then favours physical condensation rather than carbamate formation (Vieillard et al., 2018, Sneddon et al., 2014, Yu et al., 2012).

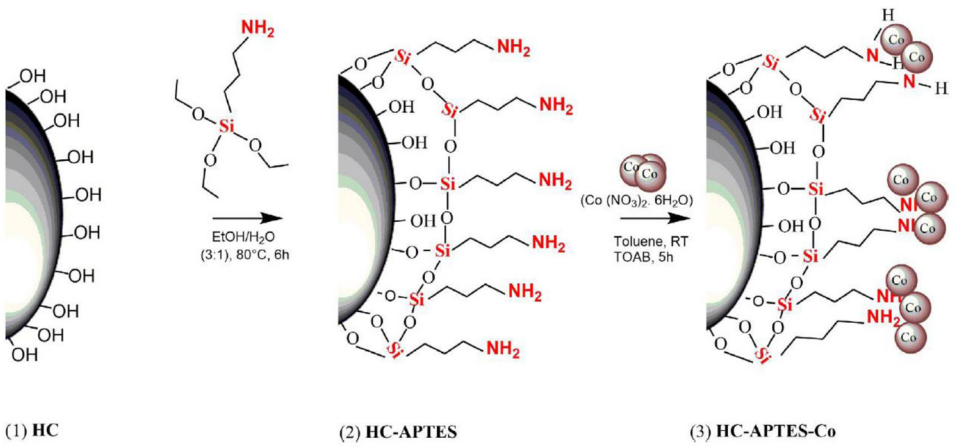

Figure 6. Schematic illustration of HC-APTES-Co preparation procedure reproduced from (Vieillard et al., 2018).

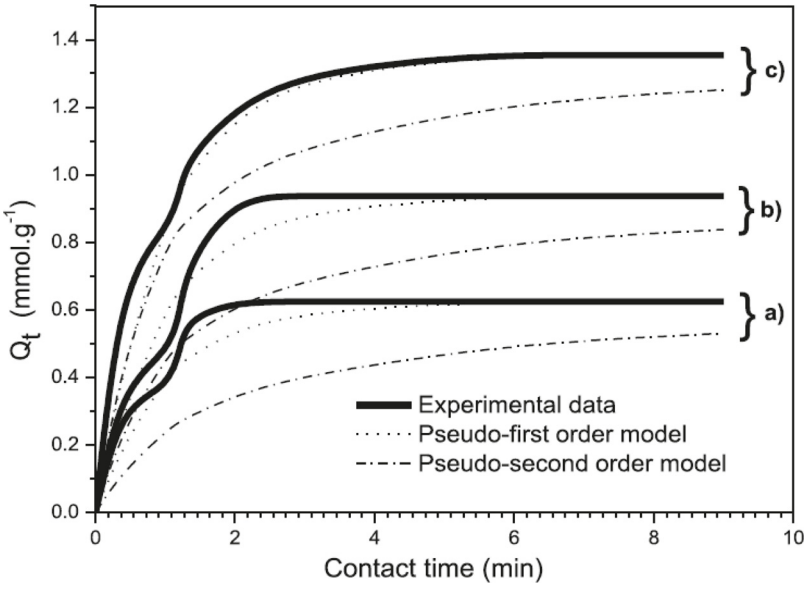

Figure 7. CO_2 adsorption kinetics of HC, HC-APTES and HC-APTES-Co under ambient temperature and pressure with pseudo-first and pseudo-second order kinetic models, reproduced from (Vieillard et al., 2018).

5. The Employment of Monte Carlo Simulations and Density Functional Theory for Evaluation of Surface Functional Group Impacts on CO_2 Adsorption

Density Functional Theory (DFT) is often used to calculate surface electronic properties of adsorbents such as atomic charges and adsorption energies. It can also be used to optimise the geometry of the models. Contrastingly, Grand Canonical Monte Carlo (GCMC) is a simulation technique, that within the context of CCS, is commonly employed to evaluate the adsorption capacity across a variety of conditions. Myriad calculations and simulations have been carried out in order to improve the understanding of carbonaceous adsorbent functionalisation, the SFGs beneficial for CO_2 adsorption, and their individual impact on the adsorption capacity.

One of the more classical SFGs studied in the realm of CCS is the amino group, due to its high Lewis basicity and the wide adoption of MEA as the industrial post-combustion CCS solvent. This functionalisation has been shown to result in an uptake of 25.94 mmol g^{-1} at 298 K and 2 MPa, and a CO_2/N_2 selectivity of 49. These results constitute a 5-fold increase in the equilibrium adsorption capacity and approximately 12-fold for the selectivity, when compared to the parent nanoporous carbon (Zhou et al., 2017). The heat of adsorption was calculated to be 34.252 kJ mol^{-1}, a significant increase from the 24.63 kJ mol^{-1} presented by the pristine sorbent. Graphene nanoribbons have also been studied *via* DFT and GCMC (Dasgupta et al., 2015). The investigation shed light onto the heat of adsorption at a pressure of 1 bar for the nitro group at 11.1 kJ mol^{-1}, and 10.52 kJ $mol^{-1}$for the amine group. The CO_2 binding energies (E_b) were calculated to be -10.74 kJ mol^{-1} and -14.69 kJ mol^{-1} for the nitro and amino SFG, respectively, and 9.89 kJ $mol^{-1}$for the parent carbon. Other N-containing functionalities, such as toluene, pyrimidine, imidazole, pyridine and etc., have been simulated as functionalised linkers of porous aromatic frameworks (PAFs) over a pressure range of 0 – 60 bar and at temperatures of 0, 25, and 50°C (Fraccarollo et al., 2014). The pyrimidine-modified sorbent has demonstrated a capacity increase of 250 % over the pristine PAF at 1 bar. Aminomethyl and tolyl SFGs also presented an improved performance to that of the parent material. The imidazole group was less efficient and demonstrated poor adsorptive properties. The positive effect of the pyrimidine functionalisation though, reduces drastically when the pressure is increased over approximately 10 bar, as this sorbent along with the other simulated functionalities performed more poorly than the unmodified material. Only the aminomethyl modification positively impacted CO_2 adsorption consistently across the investigated pressure range. Thus, pyrimidine-PAF is preferred for low pressure applications such as post-combustion capture. For high pressure applications such as gas storage the unmodified sorbent would be more appropriate; NH_2-CH_2-PAF would constitute a compromise (Fraccarollo et al., 2014). In the same study, variation of SFG loading and the impact on CO_2 adsorption uptake was also investigated. The authors demonstrated an increase in the adsorbed amount when increasing the SFG loading in low to in-

termediate pressure ranges *i.e.* below 10 to 15 bar. However, the trend is reversed at elevated pressures, so that the absolute uptake at 100 % substitution is much less than the 50% substitution (Fraccarollo et al., 2014). Other nitrogen-containing functionalities such as quaternary, pyridinic and the oxidised pyridinic-N, have been evaluated by Psarras *et al.* (Psarras et al., 2016), with the latter demonstrating a remarkable capacity for CO_2 adsorption *i.e.* 4.31 mmol g^{-1} (CO_2/N_2 selectivity of 138.3) compared to the 2.19 mmol g^{-1} (CO_2/N_2 selectivity of 24.5) of the unmodified surface under ambient conditions.

Phosphorous-containing functional groups have also been considered in the literature (Chen et al., 2021). A -C_3-P functionalised graphite was shown to have an adsorption capacity of 12.3 mmol cm^{-3} at 16 kPa, whereas at 300 kPa the material adsorbed 15.3 mmol cm^{-3}. Incorporation of SFGs such as -C-O-$PO(OH)_2$, -C_3-P and -C_3-P=O, has been shown to lead to an enhanced CO_2 uptake with energies of adsorption of -34.42 kJ mol^{-1}, -28.73 kJ mol^{-1} and -26.29 kJ mol^{-1}, respectively. These numbers show a greater affinity towards CO_2 than that of amino-functionalised graphite (adsorption energy of -18.18 kJ mol^{-1}). The SFG SO_3H has been shown to possess an adsorption energy of -33.78 kJ mol^{-1}, similar to those of the P-functionalised materials. This thio-functionalisation has been widely investigated. It was shown *via* GCMC simulations, that SO_3H functionalisation of melamine-based porous polyamides (MPPA) leads to an equilibrium capacity of 5.38 mmol g^{-1} at 1 bar and 25°C, which is higher than that of fluorine, hydroxyl, epoxy and carbonyl functionalised analogues and the parent MPPA (Song et al., 2021). Similar improvements to the CO_2/N_2 selectivity of the sorbent were also demonstrated. Additionally, S-doping of the framework itself has been evaluated *via* DFT and GCMC for its efficacy for CCS (Li et al., 2017). In this study a graphite slit pore containing 33.12 % sulphur presented heats of adsorption equal to 41.01 kJ $mol^{-1}$and a CO_2 uptake of 51 mmol mol^{-1} (at 1 bar and 27°C), constituting a 45.12 % and 39.85 % rise, respectively, when compared to a simple graphite pore. They have also demonstrated an increased affinity between CO_2 and the adsorbent when increasing the presence of heteroatoms in the framework. The material with a sulphur content of 7.94 wt% presented an improved performance over the parent material yet significantly worse than the adsorbent with the maximum doping described in the previous sentence with respect to both heat of adsorption and capacity. Not only graphite slit pores, but also 3D covalent organic frameworks (COFs) have been simulated *via* DFT and GCMC (Yuan et al., 2021). SO_3H has been denoted as the most promising SFG of those studied (OH, OCH_3, NH_2, CH_2NH_2, COOH and etc.) due to its large selectivity over nitrogen, with an E_b of -25.527 kJ mol^{-1}. However, of the investigated SFGs a rather exotic ester-carboxylic terminal group (-OOC-CH-$(CH_2)_2$-COOH) had the highest E_b -34.249 kJ mol^{-1}as well as CO_2 uptake. Interestingly, when reducing the ester chain to its alkyl analogue, the affinity towards CO_2 dropped drastically. Additionally, they also identified the pore volume being a limiting factor in CO_2 adsorption at elevated pressures. Thus, “bulky”, sterically-hindered SFGs might affect the uptake of the material rendering them useless for high pressure applications, as their capacities are lower/comparable to that of the bare COF. Hydroxyl functionalisation of the COF, on the other hand, enhanced the capacity at higher pressures. A similarly-modified AC surface has been evaluated in comparison to other O-SFGs as well as the homogenous sorbent (Yuan et al., 2020). OH-functionalisation increased the CO_2/N_2 selectivity, CO_2 heat of adsorption and uptake when averaged across a range of temperatures at ambient pressure by 432 %, 35.3% and 12.5%, respectively, compared to the pristine surface. Additionally, both the ether and ester SFGs did not improve the adsorptive properties, the latter actually hindered sorption due to pore plugging. Contrastingly, carboxylic terminal groups have been demonstrated to promote adsorption to a greater extent than the hydroxyl group within the pressure range of 0 – 2 MPa. Furthermore, heats of adsorption of 30.704 vs 30.339 kJ $mol^{-1}$and selectivity over nitrogen of ~29 vs ~15 for carboxylic and hydroxyl SFGs, respectively at 298 K and 1 MPa for nanoporous carbons (Zhou et al., 2017). Contrastingly, the heat adsorption, selectivity and equilibrium CO_2 capacity were shown to be inferior to that of the amino-functionalised material. A similar trend was observed for functionalised graphene nanoribbons at 1 bar (-COOH = 13.47 and -OH = 10.24 kJ mol^{-1}) (Dasgupta et al., 2015). Additionally, the E_b was calculated to be -15.74 and -12.10 kJ mol^{-1}, respectively. The carboxyl-functionalisation of the graphene nanoribbons yielded an increase in selectivity of 28% over the non-functionalised material (Dasgupta et al., 2015), whereas a different investigation demonstrated a drop for the functionalised adsorbents' selectivity across all of the investigated SFGs (-NH_2, -COOH and -OH) when the molar fraction of CO_2 is increased (Zhou et al., 2017). Nevertheless, oxygen-containing species are generally considered to be beneficial for CCS, since the O atoms of these SFGs (being more electronegative than the carbon framework) have a large negative partial charge (-0.9969 for hydroxyls and -1.047 for carbonyls (Liu and Wilcox, 2012)) and, thus, possess the highest potential to donate electrons to the surrounding gas molecules and to attract the C atoms of CO_2. Wang *et al.* (Wang et al., 2019) reported DFT calculations that identified a synergistic effect between pyrrolic-N and O-containing groups as a result of both electrostatic and dispersion interactions. Regardless of the N-moiety, N-doping typically leads to the increase in the heat of adsorption and binding energy (Wang and Yang, 2012, Lim et al., 2016, Saha et al., 2018). Nevertheless, adsorption is governed to a great extent by the pore width and the pore volume. Therefore, these parameters must be considered when investigating the most suitable surface functionality for carbon capture *via* carbonaceous adsorbents. For instance, incorporation of -OH or =O groups onto the top graphitic layer reduces the volume of a 9.2 Å pore by approximately 40% (Liu and Wilcox, 2012). Having said this, this reduction is much less pronounced for 20 Å wide pores. Nevertheless, the presence of these SFGs has a drastic effect on the orientation of the adsorbed CO_2 molecules. In an ideal graphite slit pore the adsorbate is immobilised in parallel to the surface. However, this orientation changes if the carbonyl (perpendicular for a 9.2 Å pore and 60° for a 20 Å pore) and hydroxyl (approximately 30° for both of the simulated pore widths) SFGs are present allowing for more efficient “side-by-side” packing, thus, increasing the uptake of the carbonaceous material. At low pressures the addition of a range of SFGs has been shown to lead to enhanced adsorption regardless of the pore size (8 – 50 Å), whereas at high pressures and pore diameters over 10 Å the presence of surface heterogeneities had a significant impact on the equilibrium capacity (Chen et al., 2021).

An alternative surface modification, metal doping also has been simulated using DFT and GCMC. Nanoporous carbons (NPC) have been shown to be positively impacted when Li-ions have been added to the sorbent (Liu et al., 2018). With a partial charge on the oxygen of the chemically bound O-Li SFG being -0.839 comparable to hydroxyls, carbonyls and carboxyls but higher than the C-O-C SFG (-0.776 (Liu and Wilcox, 2012)). A stronger affinity towards CO_2 of the chemically functionalised (substituted in the NPC framework) Li was shown in comparison to the physically adsorbed Li-species, with the latter still outperforming the parent material. At ambient temperature and pressure, the sorbent with 6 covalently bound Li cations in the framework was shown to adsorb 25.93 mmol g^{-1}, approximately 10 times higher than the simulated pristine NPC. Additionally, grafting was demonstrated to yield better results than impregnation (when modifying with the same number of metal ions) and an increased amount of doped Li led to enhanced selectivity over N_2. Similar results have been acquired *via* DFT and GCMC by other researchers as well, though, over a wider range of metals (Ma et al., 2019). Their results display superior performance of the Li-doped sorbent (approximately 12.5 mmol g^{-1}) over the non-functionalised material with the equilibrium capacity of the latter being nearly 4 times smaller than that of the best modified adsorbent at ambient conditions. Other investigated metals also yielded favourable results of approximately 11.5 mmol g^{-1} for Na and 8.5 mmol g^{-1} for K at the same conditions. Additionally, the initial heat of adsorption for the metal-doped adsorbents was nearly twice as high as for the pristine carbon (46.8 kJ $mol^{-1}$with the -O-Li SFG and 24.8 kJ $mol^{-1}$with no SFGs).

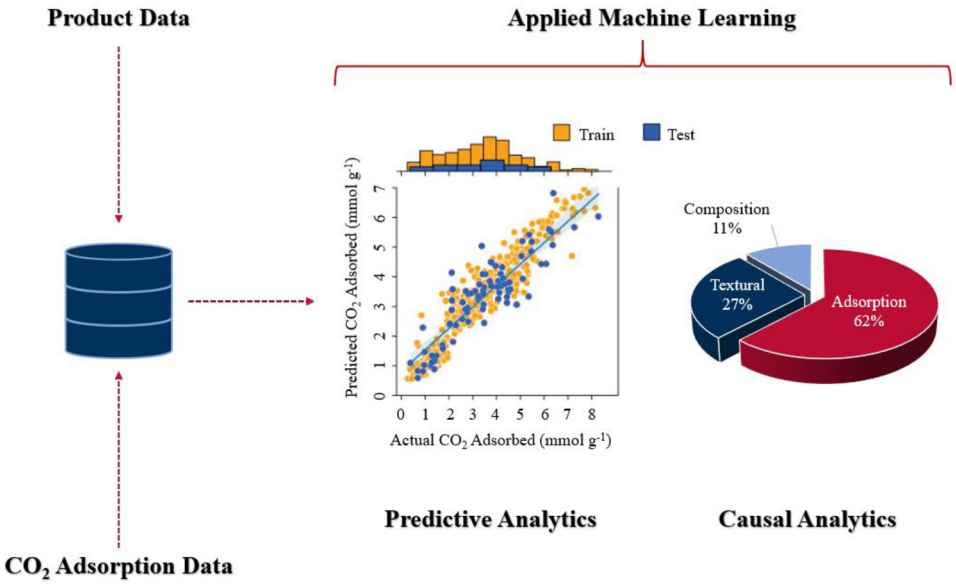

Figure 8. Workflow schematic of AI implementation reproduced from (Yuan et al., 2021).

The crucial role of the electrostatic force for Me-doped carbons was highlighted as well. Additionally, hydroxyl functionalisation was also investigated. Though leading to a higher uptake and CO_2/N_2 selectivity than that of the parent NPC, the OH functional group was shown to have a much lesser impact in comparison to the alkoxy functionalised sorbents. Others, however, have simulated a combination of these SFGs, displaying a synergistic effect of such modifications (Dang et al., 2017). When adding both the Li ions and the hydroxy radicals, such graphdiyne-based sorbents adsorbed 4.83 mmol g^{-1} at ambient conditions, nearly doubling the uptake (and the adsorption energy) of its solely hydroxyl analogue. This trend of better performance was observed below pressures of 4 MPa, where the capacities are equal for both of these materials. Interestingly, when metal doping an amino-functionalised C, a slight enhancement in CO_2 uptake over a single -NH_2 SFG is only visible up to 0.2 MPa. Above this, loss of adsorption capacity was observed. This phenomenon was attributed to a drastic reduction in ultramicropore volume due to Li-doping of the amino-sorbent. Nevertheless, the combined alkoxy-hydroxygraphdiyne adsorbent outperformed all other simulated analogues across the whole pressure range. Additionally, DFT calculations and GCMC simulations were also applied to the non-metal doped functionalised carbonaceous sorbents (Dang et al., 2017). The results indicate that CO_2 uptake at pressures below 0.4 follow the order of -NH_2 > -OH > - COOH > -F, with the latter hindering adsorption of the sorbent compared to the parent carbon. The uptake and H_{ads} at 25°C and 0.02 MPa were shown to be 1.03 mmol $^{-1}$g and 29.96 kJ mol^{-1}, 0.66 mmol g^{-1} and 29.76 kJ mol^{-1}, 0.65 mmol g^{-1} and 27.19 kJ mol^{-1}, 0.34 mmol g^{-1} and 23.84 kJ mol^{-1}, respectively, for -NH_2 > -OH > - COOH > -F functionalisation vs 0.51 mmol g^{-1} and 26.71 kJ mol^{-1} for the pristine material. These results are to be expected, due to the stronger Lewis basicity of the amino group than that of hydroxy and carboxyl groups promoting adsorption and the electron-withdrawing properties of the halogens affecting sorption of CO_2. Other investigated SFGs were the alkyne group and the phenyl ring of the graphdiyne framework. The adsorption energy above these groups was calculated to be 3.84 kJ $mol^{-1}$and 1.50 kJ mol^{-1}, respectively, suggesting the former to be more beneficial for carbon capture than the latter (Dang et al., 2017).

6. The Employment of Artificial Intelligence and Machine Learning for Evaluation of Surface Functional Group Impacts on CO_2 Adsorption

Artificial Intelligence (AI) and Machine Learning (ML) can also be exploited when investigating CO_2 adsorption properties and the influence of surface heterogeneities. Although work has been completed in the field of carbonaceous adsorbents, the quantity is far smaller than the considerable attention drawn by other and more tailorable materials such as metal-organic frameworks (MOFs). The literature suggests the separation conditions and the textural properties of the carbon-based adsorbents to be more impactful than their chemical composition (Zhu et al., 2020, Yuan et al., 2021). Zhu et al. (2020) evaluated a total of 6422 data sets from 155 porous carbon materials (PCMs) for temperatures of 0 °C and 25 °C in a pressure range up to 1 bar with nitrogen contents between 0.2 – 12.2 wt% using the Random Forest model. This model was selected due to its high accuracy, insensitivity to noise and resistance to overfitting. Of the data, 80% was selected as the training group and the final fifth were left for results validation and evaluation. The findings of their work elucidated to a far stronger impact of pore volume than that of chemical composition., a stronger impact of pore. Quantitatively this meant that the chemical composition of the sorbent was 2.3 times less influential at 0°C and a pressure between 0.6 – 1 bar than pore volume. The Pearson correlation coefficients of some of the investigated parameters were: Micropore Volume = -0.034; Mesopore Volume = -0.142; Ultramicropore Volume = 0.144; Temperature = -0.38; Pressure = 0.796, with the negative values hindering the sorption process (positive – promoting) and the modulus depicting the strength of the interaction. Thus, a weakly positive correlation between mass percentage of N (0.038) and uptake has been described. Additionally, a well-developed ML model to correlate selectivity over N_2 could not be made due to a lack of sufficient data. Nevertheless, when incorporating SFGs onto the adsorbent surface, considerations have to be made. Modelling general N-doping is not as transferrable to experimental studies as specific functionalities and does not provide sufficient insight into the sorption characteristics of the functionalised material (Figure 8).

In other works, Yuan et al. (2021) studied 527 data points, of which only 334 of 42 peer-reviewed publications described heteroatom-doped carbons at the following conditions: 0 °C and 25 °C; 0.15 bar and 1 bar. Three different tree-based models were deployed, namely, Light Gradient Boosting (LGB), Extreme Gradient Boosting (XGB) and Gradient Boosting Decision Tree (GBDT) with the latter providing the most accurate predictions. Of the evaluated data, 85% was used for training purposes, the remaining 15% was utilised for model validation. The findings showed that a carbonaceous sorbent with 10 – 14 wt% of oxygen and a N-content of 7 – 10 wt% should have a positive impact on the adsorption capacity, with the latter contributing more towards enhanced uptake than the former. This effect was ascribed to the presence of basic SFGs; however, this investigation also did not deal with spe-

cific functionalities. It is, therefore, advisable, that future investigations be focused on specific SFG impacts on the capture process in order to identify the functionalities most suitable for CCS purposes and those that affect CO_2 sorption and selectivity. The Pearson correlation matrix from Yuan et al. (2021) is largely in agreement with the findings of Zhu et al. (2020). The correlation strength between the amount adsorbed and the variables follows a similar pattern: P (0.56), T (-0.52), Surface Area (0.33), Total Pore Volume (0.29), Micropore Volume (0.27) and only then surface heterogeneities such as N (0.16) and O (-0.064). No analysis of impact of SFGs or N/O-doping was carried out.

7. Conclusion

The modification of carbonaceous adsorbents through both physical or chemical treatments is a key route to improving their associated CO_2 adsorption and thus accelerating the deployment of technologies such as adsorption based-CCS as we surmount the insurmountable challenge that is anthropogenic-induced climate change. By first considering the routes to functional group incorporation in the context of solid carbon adsorbents and then discussing the influence these may have on the adsorption of CO_2, this review has given insight into both the efficacy of surface modification techniques and the adsorption mechanisms that underpin the CO_2 removal process. The influence that specific surface functionalities may have on the adsorption of CO_2 can be seen not only in the kinetic and equilibrium performance of the porous carbon but also in the heat of adsorption. Deliberation is imperative for each when scaling-up these processes especially when one considers the energy requirement for regeneration is heavily influenced by the strength of the interaction between the adsorbate and adsorbent. Wider implementation of molecular simulations and artificial intelligence could further assist the progression of adsorption-based CCS by facilitating an accelerated understanding and prediction of adsorbate-adsorbent interaction. Significant attention still has to be paid to the effects gaseous impurities present in flue gas streams such as H_2O have on the performance of surface modified carbonaceous adsorbents; a research area that would benefit greatly from exploiting novel technologies such as molecular simulation and artificial intelligence. Deployment of full-scale adsorption-based processes relies on this comprehensive and exhaustive understanding of the adsorbent's characteristic performance under both the ideal (*i.e.* pure CO_2) and non-ideal (*i.e.* industrial flue gas) conditions with or without surface functionalities.

Declaration of Competing Interest

The authors declare that they have no known competing financial interests or personal relationships that could have appeared to influence the work reported in this paper.

Acknowledgements

This work has been funded by the UK Engineering and Physical Sciences Research Council (EPSRC) under the project titled "Multiphysics and multiscale modelling for safe and feasible CO_2 capture and storage - EP/T033940/1", and *via* the UK Carbon Capture and Storage Research Centre (EP/P026214/1) through the flexible funded research programme "Techno-economics of Biomass Combustion Products in the Synthesis of Effective Low-cost Adsorbents for Carbon Capture". The UKCCSRC is supported by the Engineering and Physical Sciences Research Council (EPSRC), UK, as part of the UKRI Energy Programme. The authors are grateful to the Research Centre for providing this funding. We would also like to acknowledge EPSRC Impact Accelerator Award (2021) for their support of this work.

Supplementary materials

Supplementary material associated with this article can be found, in the online version, at doi:10.1016/j.ccst.2022.100045.

References

Abdedayem, A, Guiza, M, Ouederni, A., 2015. Copper supported on porous activated carbon obtained by wetness impregnation: Effect of preparation conditions on the ozonation catalyst's characteristics. Comptes Rendus Chim 18 (1), 100–109.

Adelodun, AA, Kim, KH, Ngila, JC, Szulejko, J., 2015. A review on the effect of amination pretreatment for the selective separation of CO2. Appl Energy [Internet] 158, 631–642. doi:10.1016/j.apenergy.2015.08.107, Available from:.

Adsorbents, Yang RT., 2003. Fundamentals and Applications. Adsorbents: Fundamentals and Applications.

Ahmad, M, Rajapaksha, AU, Lim, JE, Zhang, M, Bolan, N, Mohan, D, et al., 2014. Biochar as a sorbent for contaminant management in soil and water: A review. Chemosphere 99, 19–33.

Ahmed, MB, Zhou, JL, Ngo, HH, Guo, W, Chen, M., 2016. Progress in the preparation and application of modified biochar for improved contaminant removal from water and wastewater. Bioresour Technol [Internet] 214, 836–851. doi:10.1016/j.biortech.2016.05.057, Available from:.

Aijaz, A, Fujiwara, N, Xu, Q., 2014. From metal-organic framework to nitrogen-decorated nanoporous carbons: High CO2 uptake and efficient catalytic oxygen reduction. J Am Chem Soc 136 (19), 6790–6793.

Alabadi, A, Razzaque, S, Yang, Y, Chen, S, Tan, B., 2015. Highly porous activated carbon materials from carbonized biomass with high CO2 capturing capacity. Chem Eng J 281, 606–612.

Alabadi, A, Razzaque, S, Yang, Y, Chen, S, Tan, B., 2015. Highly porous activated carbon materials from carbonized biomass with high CO2 capturing capacity. Chem Eng J 281, 606–612.

Alatalo, SM, Qiu, K, Preuss, K, Marinovic, A, Sevilla, M, Sillanpää, M, et al., 2016. Soy protein directed hydrothermal synthesis of porous carbon aerogels for electrocatalytic oxygen reduction. Carbon N Y 96, 622–630.

Alhwaige, AA, Agag, T, Ishida, H, Qutubuddin, S., 2013. Biobased chitosan hybrid aerogels with superior adsorption: Role of graphene oxide in CO2 capture. RSC Adv 3 (36).

Álvarez-Gutiérrez, N, Gil, M V, Rubiera, F, Pevida, C., 2017. Kinetics of CO2 adsorption on cherry stone-based carbons in CO2/CH4 separations. Chem Eng J 307, 249–257.

Arenillas, A, Smith, KM, Drage, TC, Snape, CE., 2005. CO2 capture using some fly ash-derived carbon materials. Fuel 84 (17), 2204–2210.

Babu, DJ, Bruns, M, Schneider, R, Gerthsen, D, Schneider, JJ., 2017. Understanding the influence of N-doping on the CO2 adsorption characteristics in carbon nanomaterials. J Phys Chem C 121 (1), 616–626.

Bansal, RC, Goyal, M., 2005. Activated carbon adsorption [Internet]. In: Activated Carbon Adsorption. CRC Press, pp. 1–472 Available from:.

Bedia, J, Rodríguez-Mirasol, J, Cordero, T., 2007. Water vapour adsorption on lignin-based activated carbons. J Chem Technol Biotechnol 82 (6).

Bell, JG, Benham, MJ, Thomas, KM., 2021. Adsorption of carbon dioxide, water vapor, nitrogen, and sulfur dioxide on activated carbon for capture from flue gases: Competitive adsorption and selectivity aspects. Energy and Fuels 35 (9), 8102–8116.

Budinova, T, Ekinci, E, Yardim, F, Grimm, A, Björnbom, E, Minkova, V, et al., 2006. Characterization and application of activated carbon produced by H3PO4 and water vapor activation. Fuel Process Technol 87 (10), 899–905.

Chandra, V, Yu, SU, Kim, SH, Yoon, YS, Kim, DY, Kwon, AH, et al., 2012. Highly selective CO2 capture on N-doped carbon produced by chemical activation of polypyrrole functionalized graphene sheets. Chem Commun 48 (5), 735–737.

Chang, YC, Chen, DH., 2006. Recovery of gold(III) ions by a chitosancoated magnetic nano-adsorbent. Gold Bull 39 (3), 98–102.

Chen, C, Kim, J, Ahn, WS., 2012. Efficient carbon dioxide capture over a nitrogen-rich carbon having a hierarchical micro-mesopore structure. Fuel 95, 360–364.

Chen, C, Kim, J, Ahn, WS., 2014. CO2capture by amine-functionalized nanoporous materials: A review. Korean J Chem Eng 31 (11), 1919–1934.

Chen, H, Guo, Y, Du, Y, Xu, X, Su, C, Zeng, Z, et al., 2021. The synergistic effects of surface functional groups and pore sizes on CO2 adsorption by GCMC and DFT simulations. Chem Eng J 415 (January), 128824.

Chen, J, Yang, J, Hu, G, Hu, X, Li, Z, Shen, S, et al., 2016. Enhanced CO2 Capture Capacity of Nitrogen-Doped Biomass-Derived Porous Carbons. ACS Sustain Chem Eng 4 (3), 1439–1445.

Chen, L, Cao, F, Sun, H., 2013. Ab initio study of the π-π Interactions between CO2 and benzene, pyridine, and pyrrole. Int J Quantum Chem 113 (20), 2261–2266.

Chen, T, Deng, S, Wang, B, Huang, J, Wang, Y, Yu, G., 2015. CO2 adsorption on crab shell derived activated carbons: Contribution of micropores and nitrogen-containing groups. RSC Adv 5 (60), 48323–48330.

Chiang, YC, Juang, RS., 2017. Surface modifications of carbonaceous materials for carbon dioxide adsorption: A review. J Taiwan Inst Chem Eng [Internet] 71, 214–234. doi:10.1016/j.jtice.2016.12.014, Available from:.

Chingombe, P, Saha, B, Wakeman, RJ., 2005. Surface modification and characterisation of a coal-based activated carbon. Carbon N Y 43 (15), 3132–3143.

Committe on Climate Change, 2019. Change C on C. Net Zero: The UK's contribution to stopping global warming. Committe on Climate Change.

Creamer, AE, Gao, B, Zhang, M., 2014. Carbon dioxide capture using biochar produced from sugarcane bagasse and hickory wood. Chem Eng J [Internet] 249, 174–179. doi:10.1016/j.cej.2014.03.105, Available from:.

Creamer, AE, Gao, B., 2016. Carbon-Based Adsorbents for Postcombustion CO2 Capture: A Critical Review. Environ Sci Technol [Internet] 50 (14), 7276–7289. doi:10.1021/acs.est.6b00627, Available from:.

Dandekar, A, Baker, RTK, Vannice, MA., 1998. Characterization of activated carbon, graphitized carbon fibers and synthetic diamond powder using TPD and DRIFTS. Carbon N Y 36 (12), 1821–1831.

Dang, Y, Guo, W, Zhao, L, Zhu, H., 2017. Porous Carbon Materials Based on Graphdiyne Basis Units by the Incorporation of the Functional Groups and Li Atoms for Superior CO2 Capture and Sequestration. ACS Appl Mater Interfaces 9 (35), 30002–30013.

Dasgupta, T, Punnathanam, SN, Ayappa, KG., 2015. Effect of functional groups on separating carbon dioxide from CO2/N2 gas mixtures using edge functionalized graphene nanoribbons. Chem Eng Sci 121, 279–291.
Deng, S, Ting, YP., 2005. Fungal biomass with grafted poly(acrylic acid) for enhancement of Cu(II) and Cd(II) biosorption. Langmuir 21 (13), 5940–5948.
Denis, PA., 2013. Concentration dependence of the band gaps of phosphorus and sulfur doped graphene. Comput Mater Sci 67, 203–206.
Diez, MA, Alvarez, R, Fernández, M., 2012. Biomass derived products as modifiers of the rheological properties of coking coals. Fuel 96, 306–313.
Dindi, A, Quang, DV, Nashef, E, Zahra, MRMA., 2017. Effect of PEI Impregnation on the CO2 Capture Performance of Activated Fly Ash. Energy Procedia [Internet] 114 (November 2016), 2243–2251. doi:10.1016/j.egypro.2017.03.1361, Available from:.
Do, DD., 1998. Adsorption Analysis: Equilibria and Kinetics [Internet]. Chemical Engineering 2, 913. Available from http://ebooks.worldscinet.com/ISBN/9781860943829/9781860943829.html .
Dubinin, MM., 1975. In: Progress in membrane and surface science. by DA Cadenhead, 9. Acad Press, New York, pp. 1–70.
Dubinin, MM., 1989. Fundamentals of the theory of adsorption in micropores of carbon adsorbents: Characteristics of their adsorption properties and microporous structures. Carbon N Y 27 (3), 457–467.
Ello, AS, De Souza, LKC, Trokourey, A, Jaroniec, M., 2013. Development of microporous carbons for CO2 capture by KOH activation of African palm shells. J CO2 Util 2, 35–38.
Fashi, F, Ghaemi, A, Behroozi, AH., 2020. Piperazine impregnation on Zeolite 13X as a novel adsorbent for CO2 capture: experimental and modeling. Chem Eng Commun [Internet] 1–17. doi:10.1080/00986445.2020.1746657, Available from:.
Figueiredo, JL, Pereira, MFR, Freitas, MMA, Órfão, JJM., 1999. Modification of the surface chemistry of activated carbons. Carbon N Y 37 (9), 1379–1389.
Fraccarollo, A, Canti, L, Marchese, L, Cossi, M., 2014. Monte Carlo modeling of carbon dioxide adsorption in porous aromatic frameworks. Langmuir 30 (14), 4147–4156.
Franchi, RS, Harlick, PJEE, Sayari, A., 2005. Applications of pore-expanded mesoporous silica. 2. Development of a high-capacity, water-tolerant adsorbent for CO2. Ind Eng Chem Res [Internet] 44 (21), 8007–8013. OctAvailable from: https://pubs.acs.org/doi/10.1021/ie0504194 .
Fuente, E, Menéndez, JA, Suárez, D, Montes-Morán, MA., 2003. Basic surface oxides on carbon materials: A global view. Langmuir 19 (8), 3505–3511.
García, S, Gil, M V, Martín, CF, Pis, JJ, Rubiera, F, Pevida, C., 2011. Breakthrough adsorption study of a commercial activated carbon for pre-combustion CO2 capture. Chem Eng J 171 (2), 549–556.
Goel, C, Bhunia, H, Bajpai, PK., 2015. Resorcinol-formaldehyde based nanostructured carbons for CO2 adsorption: Kinetics, isotherm and thermodynamic studies. RSC Adv 5 (113), 93563–93578.
González, AS, Plaza, MG, Rubiera, F, Pevida, C., 2013. Sustainable biomass-based carbon adsorbents for post-combustion CO2 capture. Chem Eng J 230.
Gorbounov M, Petrovic B, Lahiri A, Masoudi Soltani S. Application of Nanoporous Carbon, Extracted from Biomass Combustion Ash, in CO2 Adsorption; Application of Nanoporous Carbon, Extracted from Biomass Combustion Ash, in CO2 Adsorption. 2021;
Grondein, A, Bélanger, D., 2011. Chemical modification of carbon powders with aminophenyl and aryl-aliphatic amine groups by reduction of in situ generated diazonium cations: Applicability of the grafted powder towards CO2 capture. Fuel 90 (8), 2684–2693.
Guo, Y, Rockstraw, DA., 2007. Physicochemical properties of carbons prepared from pecan shell by phosphoric acid activation. Bioresour Technol 98 (8), 1513–1521.
Guo, Y, Tan, C, Sun, J, Li, W, Zhang, J, Zhao, C., 2020. Porous activated cartbons derived from waste sugarcane bagasse for CO2 adsorption. Chem Eng J [Internet] 381 (July 2019), 122736. doi:10.1016/j.cej.2019.122736, Available from:.
Han, KK, Zhou, Y, Chun, Y, Zhu, JH., 2012. Efficient MgO-based mesoporous CO 2 trapper and its performance at high temperature. J Hazard Mater 203–204, 341–347.
Hao, GP, Jin, ZY, Sun, Q, Zhang, XQ, Zhang, JT, Lu, AH., 2013. Porous carbon nanosheets with precisely tunable thickness and selective CO2 adsorption properties. Energy Environ Sci 6 (12), 3740–3747.
Hao, GP, Li, WC, Qian, D, Lu, AH., 2010. Rapid synthesis of nitrogen-doped porous carbon monolith for CO2 capture. Adv Mater 22 (7), 853–857.
Harlick, PJE, Sayari, A., 2006. Applications of pore-expanded mesoporous silicas. 3. Triamine silane grafting for enhanced CO2 adsorption. Ind Eng Chem Res 45 (9), 3248–3255.
Hirst, EA, Taylor, A, Mokaya, R., 2018. A simple flash carbonization route for conversion of biomass to porous carbons with high CO2 storage capacity. J Mater Chem A 6 (26), 12393–12403.
Hosseini, S, Bayesti, I, Marahel, E, Eghbali, F, Eghbali Babadi, F, Chuah Abdullah, L, et al., 2015. Adsorption of carbon dioxide using activated carbon impregnated with Cu promoted by zinc. J Taiwan Inst Chem Eng [Internet] 52, 109–117. doi:10.1016/j.jtice.2015.02.015, Available from:.
Hosseini, S, Eghbali, F, Masoudi, S, Eghbali Babadi, F, Masoudi Soltani, S, Aroua, MK, et al., 2017. Carbon dioxide adsorption on nitrogen-enriched gel beads from calcined eggshell/sodium alginate natural composite. Process Saf Environ Prot [Internet] 109, 387–399. doi:10.1016/j.psep.2017.03.021, Available from:.
Houshmand, A, Daud, WMAW, Shafeeyan, MS., 2011. Exploring potential methods for anchoring amine groups on the surface of activated carbon for CO2 adsorption. Sep Sci Technol [Internet] 46 (7), 1098–1112. Apr 28Available from: https://www.tandfonline.com/doi/abs/10.1080/01496395.2010.546383 .
Houshmand, A, Shafeeyan, MS, Arami-Niya, A, Daud, WMAW., 2013. Anchoring a halogenated amine on the surface of a microporous activated carbon for carbon dioxide capture. J Taiwan Inst Chem Eng 44 (5), 774–779.
Hu, H, Zhang, T, Yuan, S, Tang, S., 2017. Functionalization of multi-walled carbon nanotubes with phenylenediamine for enhanced CO2 adsorption. Adsorption 23 (1), 73–85.
Hu, X, Radosz, M, Cychosz, KA, Thommes, M., 2011. CO 2-filling capacity and selectivity of carbon nanopores: Synthesis, texture, and pore-size distribution from quenched-solid density functional theory (QSDFT). Environ Sci Technol 45 (16).
Jansen, RJJ, van Bekkum, H., 1994. Amination and ammoxidation of activated carbons. Carbon N Y 32 (8), 1507–1516.
Jansen, RJJ, van Bekkum, H., 1995. XPS of nitrogen-containing functional groups on activated carbon. Carbon N Y 33 (8), 1021–1027.
Jiang, J, Zhang, L, Wang, X, Holm, N, Rajagopalan, K, Chen, F, et al., 2013. Highly ordered macroporous woody biochar with ultra-high carbon content as supercapacitor electrodes. Electrochim Acta 113, 481–489.
Kast, W., 1985. Principles of adsorption and adsorption processes. Chem Eng Process Process Intensif 19 (2), 118.
Kazarian, SG, Vincent, MF, Bright, F V, Liotta, CL, Eckert, CA., 1996. Specific intermolecular interaction of carbon dioxide with polymers. J Am Chem Soc 118 (7), 1729–1736.
Kiciński, W, Szala, M, Bystrzejewski, M., 2014. Sulfur-doped porous carbons: Synthesis and applications. Carbon N Y 68, 1–32.
Kishor, R, Ghoshal, AK., 2016. Polyethylenimine functionalized as-synthesized KIT-6 adsorbent for highly CO2/N2 selective separation. Energy and Fuels 30 (11), 9635–9644.
Knaebel, KS., 2008. Albright's Chemical Engineering Handbook [Internet]. In: Albright's Chemical Engineering Handbook. CRC Press, pp. 1120–1170 Available from:.
Lahaye, J., 1998. The chemistry of carbon surfaces. Fuel 77 (6), 543–547.
Laheäär, A, Delpeux-Ouldriane, S, Lust, E, Béguin, F, 2014. Ammonia Treatment of Activated Carbon Powders for Supercapacitor Electrode Application. J Electrochem Soc 161 (4), A568–A575.
Lahijani, P, Mohammadi, M, Mohamed, AR., 2018. Metal incorporated biochar as a potential adsorbent for high capacity CO2 capture at ambient condition. J CO2 Util [Internet] 26 (January), 281–293. doi:10.1016/j.jcou.2018.05.018, Available from:.
Lee, SY, Park, SJ., 2015. A review on solid adsorbents for carbon dioxide capture. J Ind Eng Chem 23, 1–11.
Lehmann, J, Joseph, S., 2012. Biochar for environmental management: Science and technology. Biochar for Environmental Management: Science and Technology 1–416.
Li, M, Xiao, R., 2019. Preparation of a dual Pore Structure Activated Carbon from Rice Husk Char as an Adsorbent for CO2 Capture. Fuel Process Technol 186, 35–39.
Li, X, Xue, Q, Chang, X, Zhu, L, Ling, C, Zheng, H., 2017. Effects of Sulfur Doping and Humidity on CO2 Capture by Graphite Split Pore: A Theoretical Study. ACS Appl Mater Interfaces 9 (9), 8336–8343.
Li, Y, Shao, J, Wang, X, Deng, Y, Yang, H, Chen, H, 2014. Characterization of modified biochars derived from bamboo pyrolysis and their utilization for target component (furfural) adsorption. Energy and Fuels 28 (8), 5119–5127.
R. B. Bird, W. E. Stewart Lightfoo, RBBWESEN, Bird, RB, Stewart, WE, Lightfoot, EN, Lightfoot, E.N., 1960. Transport phenomena John Wiley and Sons, Inc., New York. R. B. Bird, W. E. Stewart780 pages.$11.50. AIChE J [Internet]. 1961 Jun;7(2):5J-6J. Available from: http://doi.wiley.com/10.1002/aic.690070245 .
Lim, G, Lee, KB, Ham, HC., 2016. Effect of N-Containing Functional Groups on CO2 Adsorption of Carbonaceous Materials: A Density Functional Theory Approach. J Phys Chem C 120 (15), 8087–8095.
Lin, Z, Waller, G, Liu, Y, Liu, M, Wong, CP., 2012. Facile synthesis of nitrogen-doped graphene via pyrolysis of graphene oxide and urea, and its electrocatalytic activity toward the oxygen-reduction reaction. Adv Energy Mater 2 (7), 884–888.
Lindsey, R., 2020. Climate Change: Atmospheric Carbon Dioxide [Internet]. Understanding Climate Change. Available from: https://www.climate.gov/news-features/understanding-climate/climate-change-atmospheric-carbon-dioxide .
Liu, L, Deng, QF, Hou, XX, Yuan, ZY., 2012. User-friendly synthesis of nitrogen-containing polymer and microporous carbon spheres for efficient CO 2 capture. J Mater Chem 22 (31), 15540–15548.
Liu, S, Yang, P, Wang, L, Li, Y, Wu, Z, Ma, R, et al., 2019. Nitrogen-doped porous carbons from lotus leaf for CO2 capture and supercapacitor electrodes. Energy and Fuels 33 (7), 6568–6576.
Liu, WJ, Jiang, H, Tian, K, Ding, YW, Yu, HQ., 2013. Mesoporous carbon stabilized MgO nanoparticles synthesized by pyrolysis of MgCl2 preloaded waste biomass for highly efficient CO2 capture. Environ Sci Technol 47 (16), 9397–9403.
Liu, WJ, Jiang, H, Yu, HQ., 2015. Development of Biochar-Based Functional Materials: Toward a Sustainable Platform Carbon Material. Chemical Reviews 115, 12251–12285.
Liu, X, Wei, S, Zhou, S, Wu, Z, Wang, M, Wang, Z, et al., 2018. Li-modified nanoporous carbons for high-performance adsorption and separation of CO2 over N2: A combined DFT and GCMC computational study. J CO2 Util 26 (June), 588–594.
Liu, Y, Wilcox, J., 2012. Molecular simulation of CO2 adsorption in micro- and mesoporous carbons with surface heterogeneity. Int J Coal Geol 104, 83–95.
Liu, Y, Wilcox, J., 2012. Effects of surface heterogeneity on the adsorption of CO 2 in microporous carbons. Environ Sci Technol 46 (3), 1940–1947.
Liu, Y, Wilcox, J., 2013. Molecular simulation studies of CO2 adsorption by carbon model compounds for carbon capture and sequestration applications. Environ Sci Technol 47 (1), 95–101.
Loganathan, S, Tikmani, M, Edubilli, S, Mishra, A, Ghoshal, AK., 2014. CO2 adsorption kinetics on mesoporous silica under wide range of pressure and temperature. Chem Eng J 256.
Lopez-Ramon, M V, Stoeckli, F, Moreno-Castilla, C, Carrasco-Marin, F., 1999. On the characterization of acidic and basic surface sites on carbons by various techniques. Carbon N Y 37 (8), 1215–1221.
Lu, W, Sculley, JP, Yuan, D, Krishna, R, Wei, Z, Zhou, HC, 2012. Polyamine-tethered porous polymer networks for carbon dioxide capture from flue gas. Angew Chemie - Int Ed 51 (30), 7480–7484.
Lua, AC, Lau, FY, Guo, J., 2006. Influence of pyrolysis conditions on pore development of oil-palm-shell activated carbons. J Anal Appl Pyrolysis 76 (1–2), 96–102.

Luo, Y, Zhang, S, Ma, Y, Wang, W, Tan, B, 2013. Microporous organic polymers synthesized by self-condensation of aromatic hydroxymethyl monomers. Polym Chem 4 (4), 1126–1131.

Ma, X, Li, L, Chen, R, Wang, C, Li, H, Wang, S., 2018. Heteroatom-doped nanoporous carbon derived from MOF-5 for CO 2 capture. Appl Surf Sci [Internet] 435, 494–502. doi:10.1016/j.apsusc.2017.11.069, Available from:.

Ma, X, Li, L, Chen, R, Wang, C, Zhou, K, Li, H., 2019. Doping of alkali metals in carbon frameworks for enhancing CO2 capture: A theoretical study. Fuel 236 (September 2018), 942–948.

Manyà, JJ, González, B, Azuara, M, Arner, G., 2018. Ultra-microporous adsorbents prepared from vine shoots-derived biochar with high CO2 uptake and CO2/N2 selectivity. Chem Eng J [Internet] 345 (November 2017), 631–639. doi:10.1016/j.cej.2018.01.092, Available from:.

Martín-Martínez, JM, Torregrosa-Maciá, R, Mittelmeijer-Hazeleger, MC, 1995. Mechanisms of adsorption of CO2 in the micropores of activated anthracite. Fuel 74 (1), 111–114.

Masoudi Soltani, S, Lahiri, A, Bahzad, H, Clough, P, Gorbounov, M, Yan, Y, 2021. Sorption-enhanced Steam Methane Reforming for Combined CO2 Capture and Hydrogen Production: A State-of-the-Art Review. Carbon Capture Sci Technol [Internet] 1 (August), 100003. doi:10.1016/j.ccst.2021.100003, Available from:.

McCabe, WL, Smith, JC, Harriott, P., 1993. Unit operations of chemical engineering. Choice Reviews Online. Singapore 30 30-6200-30–6200.

McDonald, TM, D'Alessandro, DM, Krishna, R, Long, JR, 2011. Enhanced carbon dioxide capture upon incorporation of N,N′- dimethylethylenediamine in the metal-organic framework CuBTTri. Chem Sci 2 (10), 2022–2028.

McEnaney, B., 1988. Adsorption and structure in microporous carbons. Carbon N Y 26 (3), 267–274.

Menéndez-Díaz, JA, Martín-Gullón, I., 2006. Chapter 1 Types of carbon adsorbents and their production. Interface Science and Technology 7, 1–47.

Montagnaro, F, Silvestre-Albero, A, Silvestre-Albero, J, Rodríguez-Reinoso, F, Erto, A, Lancia, A, et al., 2015. Post-combustion CO_2 adsorption on activated carbons with different textural properties. Microporous Mesoporous Mater 209, 157–164.

Montes-Morán, MA, Suárez, D, Menéndez, JA, Fuente, E., 2004. On the nature of basic sites on carbon surfaces: An overview. Carbon N Y 42 (7), 1219–1225.

MORRIS, JC, WEBER, WJ, 1964. REMOVAL OF BIOLOGICALLY-RESISTANT POLLUTANTS FROM WASTE WATERS BY ADSORPTION. Advances in Water Pollution Research.

Mukherjee, A, Zimmerman, AR, Harris, W., 2011. Surface chemistry variations among a series of laboratory-produced biochars. Geoderma 163 (3–4), 247–255.

Mulgundmath, VP, Jones, RA, Tezel, FH, Thibault, J., 2012. Fixed bed adsorption for the removal of carbon dioxide from nitrogen: Breakthrough behaviour and modelling for heat and mass transfer. Sep Purif Technol 85, 17–27.

Nakao, S, Yogo, K, Goto, K, Kai, T, Yamada, H., 2019. Advanced CO2 capture technologies: Absorption, adsorption, and membrane separation methods [Internet]. Book. Springer International Publishing, Cham, pp. 1–90 Available from:.

Nelson, MR, Borkman, RF., 1998. Ab initio calculations on CO2 binding to carbonyl groups. J Phys Chem A 102 (40), 7860–7863.

Nguyen, MV, Lee, BK., 2016. A novel removal of CO2 using nitrogen doped biochar beads as a green adsorbent. Process Saf Environ Prot [Internet] 104, 490–498. doi:10.1016/j.psep.2016.04.007, Available from:.

Nowicki, P, Kazmierczak, J, Pietrzak, R., 2015. Comparison of physicochemical and sorption properties of activated carbons prepared by physical and chemical activation of cherry stones. Powder Technol 269, 312–319.

Nowicki, P, Pietrzak, R, Wachowska, H., 2009. Influence of the precursor metamorphism degree on preparation of nitrogen-enriched activated carbons by ammoxidation and Chemical activation of coals. Energy and Fuels 23 (4), 2205–2212.

Ochedi, FO, Liu, Y, Adewuyi, YG., 2020. State-of-the-art review on capture of CO2 using adsorbents prepared from waste materials. Process Saf Environ Prot [Internet] 139, 1–25. doi:10.1016/j.psep.2020.03.036, Available from:.

Opatokun, SA, Prabhu, A, Al Shoaibi, A, Srinivasakannan, C, Strezov, V, 2017. Food wastes derived adsorbents for carbon dioxide and benzene gas sorption. Chemosphere [Internet]. 168, 326–332. doi:10.1016/j.chemosphere.2016.10.083, Available from:.

Papirer, E, Li, S, Donnet, JB, 1987. Contribution to the study of basic surface groups on carbons. Carbon N Y 25 (2), 243–247.

Patel, HA, Byun, J, Yavuz, CT., 2017. Carbon Dioxide Capture Adsorbents: Chemistry and Methods. ChemSusChem 10 (7), 1303–1317.

Pels, JR, Kapteijn, F, Moulijn, JA, Zhu, Q, Thomas, KM., 1995. Evolution of nitrogen functionalities in carbonaceous materials during pyrolysis. Carbon N Y 33 (11), 1641–1653.

Peng, AZ, Qi, SC, Liu, X, Xue, DM, Peng, SS, Yu, GX, et al., 2019. Fabrication of N-doped porous carbons for enhanced CO2 capture: Rational design of an ammoniated polymer precursor. Chem Eng J 369, 170–179.

Peng, AZ, Qi, SC, Liu, X, Xue, DM, Peng, SS, Yu, GX, et al., 2019. N-doped porous carbons derived from a polymer precursor with a record-high N content: Efficient adsorbents for CO2 capture. Chem Eng J 372, 656–664.

Petrovic B, Gorbounov M, Lahiri A, Masoudi Soltani S. Biomass Combustion Fly Ash-Derived Nanoporous Zeolites for Post-Combustion Carbon Capture; Biomass Combustion Fly Ash-Derived Nanoporous Zeolites for Post-Combustion Carbon Capture. 2021; Available from: https://ec.europa.eu/clima/policies/international/negotiations/pa

Petrovic, B, Gorbounov, M, Masoudi Soltani, S, 2020. Influence of surface modification on selective CO2 adsorption: A technical review on mechanisms and methods. Microporous Mesoporous Mater [Internet] (October), 110751. NovAvailable from: https://linkinghub.elsevier.com/retrieve/pii/S1387181120307514 .

Petrushenko, IK, Ivanov, NA, Petrushenko, KB., 2021. Theoretical investigation of carbon dioxide adsorption on Li+-decorated nanoflakes. Molecules 26 (24), 1–14.

Pevida, C, Plaza, MG, Arias, B, Fermoso, J, Rubiera, F, Pis, JJ., 2008. Surface modification of activated carbons for CO 2 capture. Appl Surf Sci 254 (22), 7165–7172.

Pierre-Louis, AM, Hausner, DB, Bhandari, N, Li, W, Kim, J, Kubicki, JD, et al., 2013. Adsorption of carbon dioxide on Al/Fe oxyhydroxide. J Colloid Interface Sci [Internet] 400, 1–10. doi:10.1016/j.jcis.2013.01.047, Available from:.

Pietrzak, R., 2009. XPS study and physico-chemical properties of nitrogen-enriched microporous activated carbon from high volatile bituminous coal. Fuel 88 (10), 1871–1877.

Plaza, MG, Pevida, C, Arenillas, A, Rubiera, F, Pis, JJ., 2007. CO2 capture by adsorption with nitrogen enriched carbons. Fuel 86 (14 SPEC. ISS), 2204–2212.

Plaza, MG, Pevida, C, Arias, B, Casal, MD, Martín, CF, Fermoso, J, et al., 2009. Different approaches for the development of low-cost co2 adsorbents. J Environ Eng 135 (6), 426–432.

Plaza, MG, Thurecht, KJ, Pevida, C, Rubiera, F, Pis, JJ, Snape, CE, et al., 2013. Influence of oxidation upon the CO2 capture performance of a phenolic-resin-derived carbon. Fuel Process Technol [Internet] 110, 53–60. doi:10.1016/j.fuproc.2013.01.011, Available from:.

Pokrzywinski, J, Aulakh, D, Verdegaal, W, Pham, VH, Bilan, H, Marble, S, et al., 2020. Dry and Wet CO2 Capture from Milk-Derived Microporous Carbons with Tuned Hydrophobicity. Adv Sustain Syst 4 (11).

Presser, V, McDonough, J, Yeon, SH, Gogotsi, Y., 2011. Effect of pore size on carbon dioxide sorption by carbide derived carbon. Energy Environ Sci 4 (8), 3059–3066.

Psarras, P, He, J, Wilcox, J., 2016. Molecular simulations of nitrogen-doped hierarchical carbon adsorbents for post-combustion CO2 capture. Phys Chem Chem Phys 18 (41), 28747–28758.

Psarras, P, He, J, Wilcox, J., 2017. Effect of Water on the CO2 Adsorption Capacity of Amine-Functionalized Carbon Sorbents. Ind Eng Chem Res 56 (21), 6317–6325.

Querejeta, N, Plaza, MG, Rubiera, F, Pevida, C., 2016. Water vapor adsorption on biomass based carbons under post-combustion Co2 capture conditions: Effect of post-treatment. Materials (Basel) 9 (5).

Rabbani, MG, El-Kaderi, HM., 2011. Template-free synthesis of a highly porous benzimidazole-linked polymer for CO2 capture and H2 storage. Chem Mater 23 (7), 1650–1653.

Raganati, F, Alfe, M, Gargiulo, V, Chirone, R, Ammendola, P., 2019. Kinetic study and breakthrough analysis of the hybrid physical/chemical CO2 adsorption/desorption behavior of a magnetite-based sorbent. Chem Eng J 372, 526–535.

Raganati, F, Chirone, R, Ammendola, P., 2020. CO2 Capture by Temperature Swing Adsorption: Working Capacity As Affected by Temperature and CO2 Partial Pressure. Ind Eng Chem Res 59 (8), 3593–3605.

Rajapaksha, AU, Chen, SS, Tsang, DCW, Zhang, M, Vithanage, M, Mandal, S, et al., 2016. Engineered/designer biochar for contaminant removal/immobilization from soil and water: Potential and implication of biochar modification. Chemosphere [Internet] 148, 276–291. doi:10.1016/j.chemosphere.2016.01.043, Available from:.

Rashidi, NA, Yusup, S., 2016. An overview of activated carbons utilization for the post-combustion carbon dioxide capture. J CO2 Util [Internet] 13, 1–16. doi:10.1016/j.jcou.2015.11.002, Available from:.

Ravikovitch, PI, Vishnyakov, A, Russo, R, Neimark, A V, 2000. Unified approach to pore size characterization of microporous carbonaceous materials from N2, Ar, and CO2 adsorption isotherms. Langmuir 16 (5), 2311–2320.

Regmi, P, Garcia Moscoso, JL, Kumar, S, Cao, X, Mao, J, Schafran, G, 2012. Removal of copper and cadmium from aqueous solution using switchgrass biochar produced via hydrothermal carbonization process. J Environ Manage 109, 61–69.

Ren, W, Saito, R, Gao, L, Zheng, F, Wu, Z, Liu, B, et al., 2010. Edge phonon state of mono- and few-layer graphene nanoribbons observed by surface and interference co-enhanced Raman spectroscopy. Phys Rev B - Condens Matter Mater Phys 81 (3).

Renssen, S., 2022. The hydrogen solution? Nat Clim Chang [Internet] doi:10.1038/s41558-020-0891-0, Available from:.

Rouquerol, J, Rouquerol, F, Llewellyn, P, Maurin, G, Sing, KSW., 2013. Adsorption by Powders and Porous Solids: Principles, Methodology and Applications: Second Edition. Adsorption by Powders and Porous Solids: Principles. Methodology and Applications: Second Edition 1–626.

Saha, D, Kienbaum, MJ., 2019. Role of oxygen, nitrogen and sulfur functionalities on the surface of nanoporous carbons in CO2 adsorption: A critical review. Microporous Mesoporous Mater [Internet] 287 (April), 29–55. doi:10.1016/j.micromeso.2019.05.051, Available from:.

Saha, D, Thorpe, R, Van Bramer, SE, Alexander, N, Hensley, DK, Orkoulas, G, et al., 2018. Synthesis of Nitrogen and Sulfur Codoped Nanoporous Carbons from Algae: Role in CO2 Separation. ACS Omega 3, 18592–18602.

Saha, D, Van Bramer, SE, Orkoulas, G, Ho, HC, Chen, J, Henley, DK., 2017. CO2 capture in lignin-derived and nitrogen-doped hierarchical porous carbons. Carbon N Y [Internet] 121, 257–266. doi:10.1016/j.carbon.2017.05.088, Available from:.

Salman, MS, Yazdi, SK, Hosseini, S, Gargari, MK., 2014. Effect of nitric acid modification on porous characteristics of mesoporous char synthesized from the pyrolysis of used cigarette filters. J Environ Chem Eng 2 (3), 1301–1308.

Samanta, A, Zhao, A, Shimizu, GKH, Sarkar, P, Gupta, R., 2012. Post-combustion CO 2 capture using solid sorbents: A review. Industrial and Engineering Chemistry Research 51, 1438–1463.

Sánchez-Sánchez, Á, Suárez-García, F, Martínez-Alonso, A, Tascón, JMD., 2014. Influence of porous texture and surface chemistry on the CO2 adsorption capacity of porous carbons: Acidic and basic site interactions. ACS Appl Mater Interfaces 6 (23), 21237–21247.

Sarmah, M, Baruah, BP, Khare, P., 2013. A comparison between CO2 capturing capacities of fly ash based composites of MEA/DMA and DEA/DMA. Fuel Process Technol [Internet] 106, 490–497. doi:10.1016/j.fuproc.2012.09.017, Available from:.

Seema, H, Kemp, KC, Le, NH, Park, SW, Chandra, V, Lee, JW, et al., 2014. Highly selective CO2 capture by S-doped microporous carbon materials. Carbon N Y 66, 320–326.

Serafin, J, Narkiewicz, U, Morawski, AW, Wróbel, RJ, Michalkiewicz, B., 2017. Highly mi-

croporous activated carbons from biomass for CO2 capture and effective micropores at different conditions. J CO2 Util 18, 73–79.
Seredych, M, Jagiello, J, Bandosz, TJ., 2014. Complexity of CO2 adsorption on nanoporous sulfur-doped carbons - Is surface chemistry an important factor? Carbon N Y 74, 207–217.
Sevilla, M, Falco, C, Titirici, MM, Fuertes, AB., 2012. High-performance CO2 sorbents from algae. RSC Adv 2 (33), 12792–12797.
Sevilla, M, Fuertes, AB., 2011. Sustainable porous carbons with a superior performance for CO2 capture. Energy Environ Sci 4 (5), 1765–1771.
Sevilla, M, Parra, JB, Fuertes, AB., 2013. Assessment of the role of micropore size and N-doping in CO2 capture by porous carbons. ACS Appl Mater Interfaces 5 (13), 6360–6368.
Sevilla, M, Valle-Vigõn, P, Fuertes, AB., 2011. N-doped polypyrrole-based porous carbons for CO2 capture. Adv Funct Mater 21 (14), 2781–2787.
Shafeeyan, MS, Daud, WMAW, Houshmand, A, Arami-Niya, A., 2011. Ammonia modification of activated carbon to enhance carbon dioxide adsorption: Effect of pre-oxidation. Appl Surf Sci 257 (9), 3936–3942.
Shafeeyan, MS, Daud, WMAW, Houshmand, A, Shamiri, A, 2010. A review on surface modification of activated carbon for carbon dioxide adsorption. J Anal Appl Pyrolysis [Internet] 89 (2), 143–151. doi:10.1016/j.jaap.2010.07.006, Available from:.
Shahkarami, S, Dalai, AK, Soltan, J., 2016. Enhanced CO2 Adsorption Using MgO-Impregnated Activated Carbon: Impact of Preparation Techniques. Ind Eng Chem Res 55 (20), 5955–5964.
Shen, W, Fan, W., 2013. Nitrogen-containing porous carbons: Synthesis and application. J Mater Chem A 1 (4), 999–1013.
Shen, W, Li, Z, Liu, Y., 2012. Surface Chemical Functional Groups Modification of Porous Carbon. Recent Patents Chem Eng 1 (1), 27–40.
Singh, G, Lakhi, KS, Ramadass, K, Kim, S, Stockdale, D, Vinu, A., 2018. A combined strategy of acid-assisted polymerization and solid state activation to synthesize functionalized nanoporous activated biocarbons from biomass for CO2 capture. Microporous Mesoporous Mater [Internet] 271 (May), 23–32. doi:10.1016/j.micromeso.2018.05.035, Available from:.
Singh, G, Lakhi, KS, Sil, S, Bhosale, S V, Kim, IY, Albahily, K, et al., 2019. Biomass derived porous carbon for CO 2 capture. Carbon N Y [Internet] 148, 164–186. doi:10.1016/j.carbon.2019.03.050, Available from:.
Singh, J, Basu, S, Bhunia, H., 2019. CO2 capture by modified porous carbon adsorbents: Effect of various activating agents. J Taiwan Inst Chem Eng [Internet] 102, 438–447. doi:10.1016/j.jtice.2019.06.011, Available from:.
Singh, J, Bhunia, H, Basu, S., 2018. CO2 adsorption on oxygen enriched porous carbon monoliths: Kinetics, isotherm and thermodynamic studies. J Ind Eng Chem [Internet] 60, 321–332. doi:10.1016/j.jiec.2017.11.018, Available from:.
Sinnott, RK, Towler, G., 2009. Chemical Engineering Design : SI edition. Butterworth-Heinemann, p. 1279.
Sneddon, G, Greenaway, A, Yiu, HHP., 2014. The potential applications of nanoporous materials for the adsorption, separation, and catalytic conversion of carbon dioxide. Adv Energy Mater 4 (10).
Song, D, Yang, L, Yang, J, Zhai, D, Sun, L, Deng, W., 2021. In silico design of new nitrogen-rich melamine-based porous polyamides applied to CO2/N2 separation. Chem Phys Lett 771 (March), 138509.
Spanjaard, D, Desjonqueres, MC., 1990. Electronic Theory of Chemisorption. In: Interaction of Atoms and Molecules with Solid Surfaces. Springer, pp. 255–323.
Srinivas, G, Burress, J, Yildirim, T., 2012. Graphene oxide derived carbons (GODCs): Synthesis and gas adsorption properties. Energy Environ Sci 5 (4), 6453–6459.
Stavitski, E, Pidko, EA, Couck, S, Remy, T, Hensen, EJM, Weckhuysen, BM, et al., 2011. Complexity behind CO2 capture on NH2-MIL-53(Al). Langmuir 27 (7), 3970–3976.
Su, F, Lu, C, Kuo, SC, Zeng, W., 2010. Adsorption of CO2 on amine-functionalized y-type zeolites. Energy and Fuels 24 (2), 1441–1448.
Sun, F, Liu, X, Gao, J, Pi, X, Wang, L, Qu, Z, et al., 2016. Highlighting the role of nitrogen doping in enhancing CO2 uptake onto carbon surfaces: a combined experimental and computational analysis. J Mater Chem A 4 (47), 18248–18252.
Suzuki, M., 1991. Adsorption engineering, Chemical engineering monographs. Elsevier Science 25, 278.
Tachikawa, H, Kawabata, H., 2009. Electronic states of defect sites of graphene model compounds: A DFT and direct molecular orbital-molecular dynamics study. J Phys Chem C 113 (18).
Tiwari, D, Goel, C, Bhunia, H, Bajpai, PK., 2016. Novel nanostructured carbons derived from epoxy resin and their adsorption characteristics for CO2 capture. RSC Adv [Internet]. 6 (100), 97728–97738. doi:10.1039/C6RA18291G, Available from:.
Tiwari, D, Goel, C, Bhunia, H, Bajpai, PK., 2017. Melamine-formaldehyde derived porous carbons for adsorption of CO2 capture. J Environ Manage 197, 415–427.
United Kingdom HM Government, 2020. The Ten Point Plan for a Green Industrial Revolution. Dep Business, Energy Ind Strateg. (November).
Vagner, C, Finqueneisel, G, Zimny, T, Burg, P, Grzyb, B, Machnikowski, J, et al., 2003. Characterization of the surface properties of nitrogen-enriched carbons by inverse gas chromatography methods. Carbon 2847–2853.
Vieillard, J, Bouazizi, N, Bargougui, R, Brun, N, Fotsing Nkuigue, P, Oliviero, E, et al., 2018. Cocoa shell-deriving hydrochar modified through aminosilane grafting and cobalt particle dispersion as potential carbon dioxide adsorbent. Chem Eng J [Internet] 342 (February), 420–428. doi:10.1016/j.cej.2018.02.084, Available from:.
Wang, H, Li, X, Cui, Z, Fu, Z, Yang, L, Liu, G, et al., 2020. Coffee grounds derived N enriched microporous activated carbons: Efficient adsorbent for post-combustion CO2 capture and conversion. J Colloid Interface Sci 578, 491–499.
Wang, L, Yang, RT., 2012. Significantly increased CO 2 adsorption performance of nanostructured templated carbon by tuning surface area and nitrogen doping. J Phys Chem C 116 (1), 1099–1106.
Wang, M, Fan, X, Zhang, L, Liu, J, Wang, B, Cheng, R, et al., 2017. Probing the role of O–containing groups in CO2 adsorption of N-doped porous activated carbon. Nanoscale 9 (44), 17593–17600.
Wang, P, Guo, Y, Zhao, C, Yan, J, Lu, P., 2017 Sep. Biomass derived wood ash with amine modification for post-combustion CO 2 capture. Appl Energy [Internet] 201 (2), 34–44. doi:10.1016/j.apenergy.2017.05.096, Available from:.
Wang, S, Tian, Z, Dai, S, Jiang, DE., 2017. Optimal Size of a Cylindrical Pore for Post–Combustion CO2 Capture. J Phys Chem C 121 (40), 22025–22030.
Wang, Y, Guo, T, Hu, X, Hao, J, Guo, Q., 2020. Mechanism and kinetics of CO2 adsorption for TEPA- impregnated hierarchical mesoporous carbon in the presence of water vapor. Powder Technol 368.
Wang, Y, Hu, X, Hao, J, Ma, R, Guo, Q, Gao, H, et al., 2019. Nitrogen and Oxygen Codoped Porous Carbon with Superior CO2 Adsorption Performance: A Combined Experimental and DFT Calculation Study. Ind Eng Chem Res 58 (29), 13390–13400.
Wang, Z, Zhan, L, Ge, M, Xie, F, Wang, Y, Qiao, W, et al., 2011. Pith based spherical activated carbon for CO2 removal from flue gases. Chem Eng Sci 66 (22), 5504–5511.
Webley, PA, Danaci, D., 2019. CO2 Capture by Adsorption Processes. In: Carbon Capture and Storage. Royal Society of Chemistry, pp. 106–167.
Wickramaratne, NP, Jaroniec, M., 2013. Importance of small micropores in CO2 capture by phenolic resin-based activated carbon spheres. J Mater Chem A 1 (1), 112–116.
Wilcox, J., 2012. Carbon capture. Carbon Capture 1–323.
Xia, Y, Mokaya, R, Walker, GS, Zhu, Y., 2011. Superior CO 2 adsorption capacity on N–doped, high-surface-area, microporous carbons templated from zeolite. Adv Energy Mater 1 (4), 678–683.
Xia, Y, Zhu, Y, Tang, Y., 2012. Preparation of sulfur-doped microporous carbons for the storage of hydrogen and carbon dioxide. Carbon N Y [Internet] 50 (15), 5543–5553. doi:10.1016/j.carbon.2012.07.044, Available from:.
Xiao, J, Sitamraju, S, Janik, MJ., 2014. CO2 adsorption thermodynamics over N-substituted/grafted graphanes: A DFT study. Langmuir 30 (7), 1837–1844.
Xing, W, Liu, C, Zhou, Z, Zhang, L, Zhou, J, Zhuo, S, et al., 2012. Superior CO2 uptake of N-doped activated carbon through hydrogen-bonding interaction. Energy Environ Sci 5 (6), 7323–7327.
Xu, X, Kan, Y, Zhao, L, Cao, X., 2016. Chemical transformation of CO2 during its capture by waste biomass derived biochars. Environ Pollut [Internet] 213, 533–540. doi:10.1016/j.envpol.2016.03.013, Available from:.
Yang, GX, Jiang, H., 2014. Amino modification of biochar for enhanced adsorption of copper ions from synthetic wastewater. Water Res 48 (1), 396–405.
Yang, H, Yuan, Y, Tsang, SCE., 2012. Nitrogen-enriched carbonaceous materials with hierarchical micro-mesopore structures for efficient CO 2 capture. Chem Eng J [Internet] 185–186, 374–379. doi:10.1016/j.cej.2012.01.083, Available from:.
Yong, Z, Mata, V, Rodrigues, AE., 2002. Adsorption of carbon dioxide at high temperature - A review. Sep Purif Technol 26 (2–3), 195–205.
Youk, S, Hofmann, JP, Badamdorj, B, Völkel, A, Antonietti, M, Oschatz, M., 2020. Controlling pore size and pore functionality in sp2-conjugated microporous materials by precursor chemistry and salt templating. J Mater Chem A 8 (41), 21680–21689.
Younas, M, Rezakazemi, M, Daud, M, Wazir, MB, Ahmad, S, Ullah, N, et al., 2020. Recent progress and remaining challenges in post-combustion CO2 capture using metal-organic frameworks (MOFs). Prog Energy Combust Sci [Internet] 80, 100849. doi:10.1016/j.pecs.2020.100849, Available from:.
Yu, CH, Huang, CH, Tan, CS., 2012. A review of CO2 capture by absorption and adsorption. Aerosol and Air Quality Research 12.
Yuan, F, Yang, Z, Zhang, X, Tong, C, Gahungu, G, Li, W, et al., 2021. Judicious design functionalized 3D-COF to enhance CO2 adsorption and separation. J Comput Chem 42 (13), 888–896.
Yuan, X, Lee, JGJEJG, Yun, H, Deng, S, Kim, YJ, Lee, JGJEJG, et al., 2020. Solving two environmental issues simultaneously: Waste polyethylene terephthalate plastic bottle-derived microporous carbons for capturing CO2. Chem Eng J 397 (February).
Yuan, X, Li, S, Jeon, S, Deng, S, Zhao, L, Lee, KB., 2020. Valorization of waste polyethylene terephthalate plastic into N-doped microporous carbon for CO2 capture through a one-pot synthesis. J Hazard Mater 399.
Yuan, X, Suvarna, M, Low, S, Dissanayake, PD, Lee, KB, Li, J, et al., 2021. Applied Machine Learning for Prediction of CO2Adsorption on Biomass Waste-Derived Porous Carbons. Environ Sci Technol 55 (17), 11925–11936.
Yue, L, Xia, Q, Wang, LLLLL, Wang, LLLLL, DaCosta, H, Yang, J, et al., 2018. CO2 adsorption at nitrogen-doped carbons prepared by K2CO3 activation of urea-modified coconut shell. J Colloid Interface Sci [Internet] 511, 259–267. doi:10.1016/j.jcis.2017.09.040, Available from:.
Zelenak, V, Halamova, D, Gaberova, L, Bloch, E, Llewellyn, P., 2008. Amine-modified SBA-12 mesoporous silica for carbon dioxide capture: Effect of amine basicity on sorption properties. Microporous Mesoporous Mater 116 (1–3), 358–364.
Zhang, C, Song, W, Ma, Q, Xie, L, Zhang, X, Guo, H., 2016. Enhancement of CO2 Capture on Biomass-Based Carbon from Black Locust by KOH Activation and Ammonia Modification. Energy and Fuels 30 (5), 4181–4190.
Zhang, X, Wu, J, Yang, H, Shao, J, Wang, X, Chen, Y, et al., 2016. Preparation of nitrogen-doped microporous modified biochar by high temperature CO2-NH3 treatment for CO2 adsorption: Effects of temperature. RSC Adv 6 (100), 98157–98166.
Zhang, X, Zhang, S, Yang, H, Feng, Y, Chen, Y, Wang, X, et al., 2014. Nitrogen enriched biochar modified by high temperature CO2-ammonia treatment: Characterization and adsorption of CO2. Chem Eng J [Internet] 257, 20–27. doi:10.1016/j.cej.2014.07.024, Available from:.
Zhang, X, Zhang, S, Yang, H, Shao, J, Chen, Y, Feng, Y, et al., 2015. Effects of hydrofluoric acid pre-deashing of rice husk on physicochemical properties and CO2 adsorption performance of nitrogen-enriched biochar. Energy [Internet] 91, 903–910. doi:10.1016/j.energy.2015.08.028, Available from:.
Zhang, Z, Wang, B, Sun, Q, Zheng, L., 2014. A novel method for the preparation of CO2 sorption sorbents with high performance. Appl Energy 123, 179–184.

Zhang, Z, Wang, B, Sun, Q., 2014. Fly ash-derived solid amine sorbents for CO2 capture from flue gas. In: Energy Procedia, pp. 2367–2373.
Zhao, Y, Liu, X, Yao, KX, Zhao, L, Han, Y., 2012. Superior capture of CO2 achieved by introducing extra-framework cations into N-doped microporous carbon. Chem Mater 24 (24), 4725–4734.
Zhou, S, Guo, C, Wu, Z, Wang, M, Wang, Z, Wei, S, et al., 2017. Edge-functionalized nanoporous carbons for high adsorption capacity and selectivity of CO 2 over N 2. Appl Surf Sci 410, 259–266.
Zhu, X, Tsang, DCW, Wang, L, Su, Z, Hou, D, Li, L, et al., 2020. Machine learning exploration of the critical factors for CO2 adsorption capacity on porous carbon materials at different pressures. J Clean Prod 273, 122915.
Zhu, XL, Wang, PY, Peng, C, Yang, J, Bin, Yan X, 2014. Activated carbon produced from paulownia sawdust for high-performance CO2 sorbents. Chinese Chem Lett 25 (6), 929–932.